

Rethinking Diversity in Deep Neural Network Testing

Zi Wang

University of Wisconsin-Madison
Madison, USA
zw@cs.wisc.edu

Ke Wang

Visa Research
Palo Alto, USA
kewang@visa.com

Jihye Choi

University of Wisconsin-Madison
Madison, USA
jihye@cs.wisc.edu

Somesh Jha

University of Wisconsin-Madison
Madison, USA
jha@cs.wisc.edu

ABSTRACT

Motivated by the success of traditional software testing, numerous diversity measures have been proposed for testing deep neural networks (DNNs). In this study, we propose a shift in perspective, advocating for the consideration of DNN testing as directed testing problems rather than diversity-based testing tasks. We note that the objective of testing DNNs is specific and well-defined: identifying inputs that lead to misclassifications. Consequently, a more precise testing approach is to prioritize inputs with a higher potential to induce misclassifications, as opposed to emphasizing inputs that enhance "diversity."

We derive six directed metrics for DNN testing. Furthermore, we conduct a careful analysis of the appropriate scope for each metric, as applying metrics beyond their intended scope could significantly diminish their effectiveness. Our evaluation demonstrates that (1) diversity metrics are particularly weak indicators for identifying buggy inputs resulting from small input perturbations, and (2) our directed metrics consistently outperform diversity metrics in revealing erroneous behaviors of DNNs across all scenarios.

1 INTRODUCTION

Deep learning (DL) systems have exhibited remarkable performance across a spectrum of machine learning tasks, reshaping modern society [16, 22]. Despite their widespread application, these systems still maintain a largely opaque decision process. To exacerbate the situation, they are shown susceptible to *functionality bugs* [1, 10, 32]. Here, we loosely define functionality bugs as misalignment between the ground-truth of inputs and the DNN classification results. To effectively identify such functionality bugs, this work introduces a new methodology for testing DNNs, in particular, we focus on DNN classification models as the programs under testing, given that the DNN classification problem represents a canonical task in deep learning [8]. In recent years, researchers have proposed various methods to test DNNs [6, 11, 26, 38]. Many of them are motivated by traditional software testing practices, particularly with an emphasis on improving input diversity. The underlying assumption is that diverse inputs can traverse the program more thoroughly, uncovering corner cases [7, 39].

Contrary to existing work of DNN testing, our testing framework does *not* employ the diversity heuristics. Instead, we advocate for treating DNN testing tasks in the literature [26, 38] as *directed* testing tasks. Directed testing is primarily concerned with the detection of specific bugs (Section 2.2). This approach is better suited to the

nature of DNN testing, considering that the functionality of DNNs is clear-cut — making predictions that align with human visual perception. Therefore, testing DNNs comes with a well-defined, specific objective — finding inputs that cause DNNs to mispredict (Section 2.1). Take image classification models as an example; in technical terms, this objective entails seeking inputs that lead DNNs to produce values in their logit layer such that the index of the maximum value no longer corresponds to the label of an input image. Given the precision and clarity of this testing goal, it is more appropriate to adopt a directed testing approach that prioritizes inputs that have a higher potential to trigger misclassifications by DNNs, rather than inputs that improve "diversity" [2, 34].

Inputs Transformations. Due to the substantial cost involved in obtaining and manually labeling test inputs, we opt to generate inputs through visual-semantics preserving transformations. These transformations augment existing inputs with variations such as unnoticeable noise, image rotation, shifts, and shearing [6, 30, 32] (Section 2.3). Regrettably, recent diversity-based testing works overlooked the case small noise can be applied to the inputs [6, 38]. This scenario is necessary to consider because minor distortions can arise in data acquisition systems and remain imperceptible to humans. Furthermore, these subtle distortions can lead to misclassifications by DNNs, a phenomenon widely recognized as *adversarial examples* [32]. Adversarial examples have emerged as a prominent research topic in the field of deep learning over the past few years, inspiring many influential works, including generative adversarial networks and stable diffusion models [9, 10, 27]. Consequently, testing methodologies that overlook adversarial examples risk compromising their credibility.

In contrast, our testing framework can address not only natural input transformations such as image rotation and shifts [6, 30] but also small noise. In fact, our formal analysis shows that the two types of transformations have significantly different mathematical properties despite being under the umbrella term of visual semantics preserving transformations. This distinction has a further impact on the scope of testing methods.

Moreover, we propose that testing can be expedited by leveraging an intrinsic nature of DL systems: differentiability. The differentiability of DNNs enables us to derive fast and precise linear approximations of testing metrics by utilizing gradients. As we explain later (Section 3.2), adversarial examples created by projected gradient descent (PGD) [21], state-of-the-art ℓ_p -adversarial attacks, can be instantiated from our testing framework. In essence, the

results of existing adversarial attacks can all be viewed as specific instances of the testing inputs to our framework when we only consider small ℓ_p -distortions as the input transformations.

We evaluate our claims over four datasets and three types of standard DNN architectures, in particular, we compare our framework with several diversity-based methods on both standard and metamorphic testing tasks. Our evaluation shows that when input transformation is restricted to small distortions only, our directed metrics are significantly more effective than diversity metrics in identifying inputs that induce functionality bugs in DNNs. More specifically, given the same set of test inputs, those that are highly ranked by our directed metrics consistently lead DNNs to misclassifications. In contrast, inputs that are prioritized by diversity metrics barely trigger the erroneous behavior from DNNs. Moreover, when the other type of input transformations – natural transformation – is taken into account, our directed metrics are again more effective than diversity metrics in exposing the functionality bugs of DNNs.

The core contribution of our work lies in uncovering the shortcomings of diversity metrics and highlighting the advantages of directed metrics for testing DNNs. Furthermore, we demonstrate how these directed testing metrics can be harnessed to effectively detect functionality bugs in the DNN, similar to Xie et al. [38]. It is worth noting that while our metrics may be applied to train more robust DNNs, this is not the primary focus of our work. Instead, our emphasis is to devise a general and effective framework for testing DNNs based on directed metrics.

To summarize, we make the following contributions:

- **Novelty:** We provide a novel conceptual framework for DNN functionality testing, and demonstrate that some state-of-the-art DL practices are the natural consequences of this framework; while Harel-Canada et al. [11], Pavlitskaya et al. [25] only refuted the application of neuron coverage, a specific diversity measure. Hence, we are more constructive compared to Harel-Canada et al. [11], Pavlitskaya et al. [25].
- **Formality:** We formalize the testing problem and carefully analyze the input transformations. In particular, we demonstrate that although small distortions and natural image transformations do not alter human judgment, they have distinct mathematical properties and should be addressed differently for testing purposes. We justify this distinction both theoretically and empirically. To the best of our knowledge, ours is the first work that has explicitly studied this distinction, and we assert that this nuanced examination is imperative.
- **Verifiability:** We evaluate our claims over four datasets and three types of standard DNN architectures, and open source the code and dataset needed for the evaluation.

2 BACKGROUND

2.1 Mathematical Notations and Definitions

Let $[n] = \{1, \dots, n\}$. For a vector $v \in \mathbb{R}^n$, $\text{sign}(v) \in \{-1, 0, 1\}^n$ such that

$$\text{sign}(v)_i = \begin{cases} 1, & v_i > 0 \\ 0, & v_i = 0 \\ -1, & v_i < 0 \end{cases}$$

Let $\|v\|_p$ denote the ℓ_p norm of a vector v , i.e.,

$$\|v\|_p = \sqrt[p]{\sum_{i=1}^n |v_i|^p}.$$

The canonical Euclidean norm is then $\|v\|_2$. Another commonly considered norm on the input is the ℓ_∞ -norm, defined as

$$\|v\|_\infty = \max_{i \in [n]} |v_i|.$$

For two functions f and g , $f \circ g(x) = f(g(x))$ denotes the composition of f and g . If $f : \mathbb{R}^n \rightarrow \mathbb{R}$ is differentiable, we use $D^i f$ to denote the i -th order differentiation of partial derivatives, e.g., $D^1 f$ is the gradient of f , and $D^2 f$ is the Hessian of f . As a convention, we omit 1 when we denote gradient, i.e., we use Df to denote the gradient of f .

For an infinitely differentiable multivariate function $f : \mathbb{R}^n \rightarrow \mathbb{R}$, the Taylor expansion T of f at $a \in \mathbb{R}^n$ is

$$T(a + \Delta x) = f(a) + (\Delta x)^T Df(a) + \frac{1}{2} (\Delta x)^T D^2 f(a) (\Delta x) + \dots, \quad (1)$$

Therefore, $T(a + \Delta x)$ is an infinite series. If f is analytic, then $T(a + \Delta x)$ converges to $f(a + \Delta x)$ [28]. In this work, we only work with the first two terms of T ; that is, we only consider

$$f(a) + (\Delta x)^T Df(a). \quad (2)$$

Given the information of f at a (i.e., $f(a)$ and $Df(a)$), Equation (2) is the linear approximation of f at $a + \Delta x$. This can provide an estimation of $f(a + \Delta x)$ if we do not want to evaluate f at $a + \Delta x$ directly: $f(a + \Delta x) \approx f(a) + (\Delta x)^T Df(a)$. In the supplementary materials, we illustrate a linear-approximation example in the one-dimensional case (Figure 3).

Remark 2.1. The quality of linear approximation depends on how large Δx is, and how close f is to a linear function. The smaller Δx is, the higher precision that approximation is, the closer the result of Equation (2) is to Equation (1). If f is already linear, then all the higher-order beyond linear terms become 0, and Equation (1) degenerates to Equation (2).

DNNs. We hereby discuss some basics of DNNs that are needed to elaborate our testing approach. A feed-forward DNN $f : \mathbb{R}^m \rightarrow \mathbb{R}^l$ is a composition of affine transformations and non-linear activation functions:

$$f_1(x) = W^{(1)}x + b^{(1)}; \quad f_i(x) = W^{(i)}\sigma(x) + b^{(i)}, \quad i = 2, \dots, d.$$

where $W^{(i)} \in \mathbb{R}^{n_{i+1} \times n_i}$ is the weight matrix between the layers with $n_1 = m$ and $n_{d+1} = l$, d is the depth of the network, and $b^{(i)} \in \mathbb{R}^{n_{i+1}}$ is the bias term. σ , the activation, is an element-wise non-linear function. Also, we have $f = f_d \circ \dots \circ f_1$. Notice that practical activation functions are (almost) everywhere infinitely differentiable except at one point (e.g., $x = 0$ for ReLU). However, this does not impact the validity of the linear approximation. If f is infinitely differentiable at x and Δx is small, then the f is also infinitely differentiable at the neighborhood centered at x .

Remark 2.2. In general, a neural network is highly non-linear. Therefore, when f in Equation (2) is realized as a DNN, for the linear approximation to be precise, it is necessary for Δx to be small.

In this work, our focus is on DNNs for standard classification tasks. $f : \mathbb{R}^m \rightarrow \mathbb{R}^l$ has l outputs, and let $f^{(i)}$ be the i -th output of f . The classification of an input x is $C(f, x) = \arg \max_{k \in [l]} f^{(k)}(x)$. Suppose that the prediction of x is i , then $f^{(i)}(x) > f^{(j)}(x)$ holds for all $j \neq i$. The output of f is called the logit score, and the classification model outputs the class with the highest logit score.

2.2 Software Testing

Large software artifacts have been an integral part of modern society for decades and are evolving on a constant basis. Despite its ubiquity, software usually contains various defects, and some of them can raise serious security concerns. Testing remains one of the most efficient ways to demonstrate the presence of bugs. Since modern software is complicated, bugs can occur anywhere in the program. For instance, a buffer usage in the program could potentially introduce overflow.

Diversity in Software Testing. In general, automated testing techniques are commonly guided by diversity heuristics: a diverse set of inputs can execute the program thoroughly and therefore, is likely to expose more bugs [7]. One of the diversity measures in testing is code coverage with multiple granularities encompassing function coverage, basic block coverage, and path coverage. For instance, American Fuzzy Lop (AFL), one of the most popular fuzzing tools, is a state-of-the-art *general-purpose* fuzzer that employs the coverage maximization heuristics [39]. It repeats a loop involving input mutation, execution of programs, and evaluation of coverage-based diversity metric. AFL generates inputs aiming to execute different parts of the program and has successfully detected numerous bugs in various applications.

Directed Software Testing. Unlike general-purpose software testing tools such as AFL, directed testing prioritizes inputs that are close to the *specific* testing goal. For instance, a data-race testing tool should prioritize inputs that are more likely to trigger concurrency bugs rather than inputs executing unseen parts of programs [13]. In software testing, this proximity can often be measured statically by distance in code. Specifically, inputs that trigger data-races must traverse code that can be executed concurrently, so the proximity can be measured by the distance between the current execution trace and target race conditions in the program. Accordingly, the testing objective should be mutating inputs to lead executions moving closer to the targets and eventually triggering the specific bugs [34].

Researchers have developed several directed testing tools, and shown that they are more capable of detecting specific bugs than general-purpose testing tools [2]. Inspired by these findings, in the following Section 2.3, we illustrate that the objective of DNN testing is well-defined and specific; thereby, DNN testing should conceptually be considered as directed testing.

2.3 DNN Testing

Diversity in DNN Testing. Inspired by the success of traditional software testing, the previous literature on DNN testing has been focused on devising various diversity measures. One of the first diversity measures is neuron coverage (NC) [26], similar to the code coverage in traditional software testing, which measures how many

neurons are activated above a specified threshold k . The assumption is that the more neurons are activated, the more states of DNNs are explored. Later works refined the definition of NC and proposed several structural variants of NC, including the neuron boundary coverage and strong neuron activations [20]. More recently, Xie et al. [38] proposed to use intermediate layer activation divergence between metamorphic inputs as an indicator to detect prediction violations, arguing that inputs with different intermediate activation patterns should also have divergent predictions. Gao et al. [6] proposed a measure to compute the fault pattern of inputs based on the normalized logit score, and a test selection algorithm that chooses a subset of inputs with diverse fault patterns and higher prediction uncertainty.

Testing objective. The functionality of DNNs is to classify inputs correctly aligned with human perception. Accordingly, functionality bug in the classification setting is characterized as incorrect classification, and the testing goal is to generate inputs that lead to misclassification. However, obtaining such test inputs and manually labeling them is usually a very expensive process. To address this test generation problem, metamorphic testing [4] has been proposed to augment existing inputs with metamorphic relations. Since the functionality of vision models is to align the model judgment with human perception, one important metamorphic relation is *equivalence-preserving* image transformations under the visual semantics. We refer to these transformations as visual semantics-preserving transformations. Now, instead of manually collecting and labeling new test inputs, one could simply augment the original dataset by applying a few compositions of such visual semantics-preserving transformations on labeled inputs, and labels are supposed to be retained since the semantics of inputs are preserved. If any of those transformed inputs alter the DNN's prediction, then we identify successful test inputs for *functionality testing* (i.e., test inputs that trigger misclassification).

Visual semantics-preserving transformations. There exist two types of transformations that leave human judgment on input semantics unaffected. The first type comprises *natural transformations*, such as image rotation, zooming, and brightness adjustments. The second type involves *small distortions* constrained by the ℓ_p -norm, which is popular under the name of adversarial examples in DL literature [10, 32]. Despite this, recent prominent works on diversity-based DNN testing have predominantly focused on natural transformations [38], even explicitly overlooking small distortions [6]. In this paper, we aim to propose a functionality testing framework that effectively incorporates both types of perturbations. This is achieved by approaching DNN testing as directed testing rather than diversity-based testing.

2.4 Our Main Thesis

Simple semantics of DNN. The core message of this paper is to highlight that diversity-based methods inspired by software testing are not the ideal testing framework for DNN testing focused on functionality bugs. Compared with traditional software, which might contain complicated structures like pointer aliasing, various data structures, and indirect function calls, DNNs are specialized

numerical programs only involving a few operations: matrix addition and multiplication, activation function, and the max function and vector indexing. Hence, the techniques designed to handle the complexity in traditional software might not be directly applicable to DNNs. Such observation naturally leads us to the main thesis of our work:

Functionality testing of DNNs is a directed testing task.

This is because, under the simple semantics of DNN, the mathematical description of the testing objective (*i.e.*, goal of functionality testing as described earlier in Section 2.3) can be very specified, which will be elaborated in Section 3. Furthermore, our perspective based on directed testing toward DNN testing enables addressing various input transformations (both natural transformations and small distortions), while the perspective of previous works based on diversity metrics is only effective with natural transformations.

Remark 2.3. Even if small distortions and natural image transformations are under the same umbrella term, visual semantics-preserving transformations, they are mathematically distinct transformations. Natural image transformations like image rotations can change the pixel representation of images significantly.

3 PROPOSED METRICS FOR DNN TESTING

We first combine the DNN semantics and functionality testing goal to derive the forward fitness metrics, which are suitable for natural transformations (Section 3.1). Then, we apply the linear approximation in Equation (2) to the forward fitness metrics to derive the backward counterparts using the gradients, suitable for small perturbations on images (Section 3.2). Finally, we combine both forward and backward scores to address the case where both natural input transformations and small perturbations are allowed (Section 3.3). The lesson is that the effectiveness of the fitness metrics depends on the underlying input transformations, so one needs to carefully analyze the transformations before using the metrics.

3.1 Forward Fitness

We use x to denote a human-labeled input, and let x' be a generated input from a few small visual semantics-preserving transformations, similar to input mutation in traditional software testing. We fix a DNN under test: f . Let $i \in [l]$ be x 's label. We assume that f classifies x correctly, *i.e.*, $C(f, x) = i$. Clearly, the goal of functionality testing is to identify the buggy x' so that the f 's classification over x' will change, *i.e.*, $C(f, x') \neq C(f, x)$. We provide two different interpretations of bugs, each of which can provide a testing metric.

Margin score. $C(f, x) = i$ implies $f^{(i)}(x) > f^{(j)}(x), \forall j \in [l], j \neq i$. We define

$$g_{ji} = f^{(j)} - f^{(i)},$$

where $g_{ji}(x) < 0, \forall j \neq i$, because $C(f, x) = i$. To change the prediction of f on x' that is close to x semantically, we need $f^{(j)}(x') > f^{(i)}(x')$ for some $j \in [l], j \neq i$. Hence, the fitness function for functionality testing could be

$$\max_{j \neq i} (f^{(j)}(x') - f^{(i)}(x')) = \max_{j \neq i} g_{ji}(x'), \quad (3)$$

i.e., any transformed input x' with the greatest value of $\max_{j \neq i} g_{ji}(x')$ is considered the most promising one to expose the bug. Intuitively,

the transformed input with a higher margin difference between other classes and the correct label is considered better and has a greater chance to alter the prediction. We refer to Equation (3) as *forward margin score*.

Loss score. When the network is trained, a loss is used to measure the distance between the logit score $f(x)$ and the ground truth i . The training process minimizes the loss to fit the data to the label, *i.e.*, if this measure is small, the x is likely to be classified correctly. This naturally provides a measure for the bug: if the loss is big, then x is likely to be misclassified. Based on this, we quantify how a muted input x' is likely to cause the misclassification as follows,

$$CE(f(x'), i) = -\log \frac{e^{f^{(i)}(x')}}{\sum_{j=1}^n e^{f^{(j)}(x')}}. \quad (4)$$

where we use the cross-entropy function, the most common and conventional choice of loss in classification tasks [8, chapter 3]. We refer to this score as *forward loss score*.

3.2 Backward Fitness

To collect the logit score of input x' , one has to execute the DNN on x' . This can be expensive, especially when there are many input transformations, and the model is large. However, one distinguishable characteristic of neural networks compared to traditional software is that neural networks are differentiable. Recall that Equation (2) defines a linear approximation of a function via gradients. This allows us to quickly estimate the values of the functions without executing the neural networks.

More formally, suppose we have an input x and the transformed input x' , we can define $\Delta x = x' - x$. From Equation (2), we know that $f(x') \approx f(x) + (\Delta x)^T Df(x)$. Based on this analysis, we introduce gradient-based surrogate versions of the two fitness scores proposed in Section 3.1, *i.e.*, margin score and loss score.

Surrogate margin score. For the margin score in Equation (3), the quantity we want to estimate is $g_{ji}(x')$. We can compute the value of g_{ji} at x , $g_{ji}(x)$, and the gradient at x , $Dg_{ji}(x)$, then we have

$$\bar{g}_{ji}(x') = g_{ji}(x) + (\Delta x)^T Dg_{ji}(x).$$

$\bar{g}_{ji}(x')$ is a linear approximation of the margin score $g_{ji}(x')$. Now, instead of identifying the input x' that has the greatest value of $\max_{j \neq i} (f^{(j)}(x') - f^{(i)}(x'))$ (Equation (3)), we choose the input x' that has the greatest value of

$$\max_{j \neq i} (\bar{g}_{ji}(x')). \quad (5)$$

We refer to this score as the *backward margin score*, because we need the gradient to compute this approximation, and gradient computation requires backpropagation over the computation graph.

Surrogate loss score. To approximate Equation (4) at x' , we have

$$\bar{CE}(f(x'), i) = CE(f(x), i) + (\Delta x)^T \cdot D(CE)(f(x), i), \quad (6)$$

where $D(CE)(f(x), i)$ is the gradient of the cross-entropy function at x . We refer to this score as the *backward loss score*.

Computational efficiency. Using the linear approximation surrogate is particularly beneficial when the number of transformations is huge, and the number of model parameters is much larger than

the dimensions of the inputs, which is always true for modern network architecture. We compute the gradient with the original input once, and then for every transformation, we only need to compute the difference in the input domain, which is a much cheaper operation than executing the neural network with every transformed input. In the supplementary material, we provide a running time analysis of gradient methods.

Analytical solution to linear approximation. The backward gradient surrogate can be more valuable when the transformation set is continuous and has a simple nice geometry. Because the set is continuous, theoretically, there are infinitely many transformations in the set. Therefore, forward-executing all transformed inputs becomes infeasible. However, if we use the gradient to approximate the function value, we can sometimes derive the optimal transformation among all possible ones to maximize the linear approximation in Equation (2) analytically. For instance, if the transformation set is ℓ_2 or ℓ_∞ -transformations, the geometry of the sets is either Euclidean balls or hypercubes. To maximize the gradient inner product, one only needs to project the gradient to the ℓ_p -balls. Specifically, if the perturbation set is an ℓ_2 -ball with radius ϵ , the projection of the gradient inside the ball is

$$\frac{h}{\|h\|_2} * \epsilon \quad (7)$$

where h is the gradient. If the perturbation set is an ℓ_∞ -ball with radius ϵ , then the projection of h becomes

$$\epsilon * \text{sign}(h). \quad (8)$$

Proposition 3.1. Equation (7) is the optimal solution to the linear approximation in the ℓ_2 -ball; and Equation (8) is the optimal solution to the linear approximation in the ℓ_∞ -ball.

The proof is included in the supplementary materials. This is the core idea of PGD, the state-of-the-art ℓ_p -attacks, where the gradient comes from the loss-based score, similar to Equation (6). Thus, when using gradient methods and the underlying transformation includes all small ℓ_p -perturbations, we also use the gradient to generate the analytical solutions as in Equations (7) and (8) to test DNN.

Remark 3.2. In practice, PGD is a parameterizable multi-step adaptive projection of the gradients. On ℓ_∞ -transformations, the one-step gradient projection coincides with the Fast Gradient Sign Method (FGSM) from the literature of adversarial examples [10].

3.3 Mixed Fitness

Recall that in Remark 2.2, if Δx is big, the approximation quality from gradients is poor. Therefore, we can also define a Δx -dependent metric such that, when Δx is big, we use the forward score in Section 3.1; and when Δx is small, we consider the linear approximation in 3.2. Accordingly, regarding the margin score, we define

$$MM(x') = \begin{cases} \max_{j \neq i} (g_{ji}(x')), & \|\Delta x\|_p > \epsilon \\ \max_{j \neq i} (\hat{g}_{ji}(x')), & \|\Delta x\|_p \leq \epsilon \end{cases} \quad (9)$$

which is named *mixed margin score*. Similarly, for the loss score, we have

$$ML(x') = \begin{cases} CE(f(x'), i), & \|\Delta x\|_p > \epsilon \\ \overline{CE}(f(x'), i), & \|\Delta x\|_p \leq \epsilon \end{cases} \quad (10)$$

which is named *mixed loss score*. Note that the condition decision in Equations (9) and (10) is a cheap operation. We only need to compute $\Delta x = x' - x$ and find the ℓ_p -norm of all Δx . If we only consider small ℓ_p transformations, mixed scores correspond to their gradient-score counterparts. On the contrary, if all the transformation is large, mixed scores coincide with their forward-fitness counterparts. The rationale is that gradients measure the local variation of a function around a concrete input, and provide imprecise information when the input is allowed to change significantly. In this case, we should execute the DNN on the transformed input.

Theoretical takeaway. In fact, executing the DNN provides the most precise result, and should always be considered as a baseline. In an ideal scenario with unlimited computational resources, there would be no need to rely on gradient-based linear approximations: one can simply execute all transformed inputs and identify the buggy ones. Gradient-based linear approximation, while not as precise, presents a reasonable compromise when dealing with resource limitations and the underlying input change Δx is small from Remark 2.2. PGD is the natural consequence of this approximation. However, one needs to understand the nature of input transformations to which gradient methods are applicable. Otherwise, the linear approximation can produce quite imprecise results.

4 EVALUATION

In this section, we evaluate the main claims that we made in Section 3:

1. The directed metrics are effective in exposing bugs in functionality testing;
2. Each metric is effective within its application scope and can have performance degradation outside the scope.

In addition, we conduct a comprehensive comparison between our directed metrics and diversity metrics, particularly when considering the small distortions as the input transformation, a critical aspect that has been overlooked by existing diversity-based DNN testing works [6, 38]

For most testing frameworks, the ordinal relations of mutated inputs are more important than the absolute score values. Therefore, when comparing different metrics, our primary interest lies in assessing how closely these metrics align in ranking inputs. In particular, given that our forward fitness score is derived from logit scores, evaluating the similarity between other metrics and the forward fitness score enables us to understand the correlation between other metrics and changes in logit scores. This ranking similarity serves as the foundation of our work.

We then use various metrics to test the DNNs. We consider two testing scenarios, depending on whether ground-truth labels are available. When the ground-truth labels are available, we refer to the testing scenario as *standard testing*. In standard testing, the goal is to generate inputs that cause misclassification as in the adversarial robustness literature [10, 21]. When ground-truth labels are unavailable, we refer to the testing scenario as *metamorphic testing*. In this case, the testing rationale is that even if the ground-truth label is unavailable, if two inputs are metamorphic and classified differently, then at least one of the two inputs is misclassified. This testing scenario is considered in Chen et al. [4], Xie et al. [38]. While

metamorphic testing is not standard, it still falls into the category of functionality testing because the metamorphic inputs inducing divergent classifications also trigger misclassifications.

Because the application scope is defined by the underlying input transformation, we evaluate the performances of the metrics with different types of transformations separately in all experiments.

More specifically, we want to answer the following research questions:

RQ 1: How closely do the metrics align in their ranking of the inputs?

RQ 2: Are the directed metrics induced from our framework more effective than the diversity metric for exposing bugs in DNNs in standard testing tasks?

RQ 3: Are the directed metrics induced from our framework more effective than the diversity metric for exposing bugs in DNNs in metamorphic testing tasks?

4.1 Datasets and models

We use four standard datasets. (1) MNIST [18] contains 10 classes of grayscale handwritten images with 60,000 training inputs and 10,000 inputs. (2) SVHN [24] contains 10 classes representing digits, 73257 inputs for training, 26032 digits for testing. (3) CIFAR10 [15] contains 60,000 32×32 colour images in 10 classes. There are 50000 training images and 10000 testing images. (4) CIFAR100 [15] is similar to CIFAR10, but has 100 classes containing 600 images each. There are 500 training images and 100 testing images per class. Among the four datasets, MNIST is grayscale inputs (1 channel) and the rest are RGB colorful inputs (3 channels). We use three classical architectures from the computer vision community for our experiments: LeNet-1 and LeNet-5 [17], VGG-16 [31], and ResNet-9 and ResNet-18 [12]. More details on datasets and models are summarized in Table 5 in the supplementary materials.

Input Transformations. We consider two sets of transformations on the input: (1) **small distortions (SDs)** that are specified by ℓ_∞ -balls or ℓ_2 -balls with *small* radii ϵ_∞ and ϵ_2 ; (2) **natural transformations** such as zooming and blurring [6].

Notice that natural transformations and SDs are not mutually exclusive. The difference is that for SDs, we would allow all possible small additive ℓ_p distortions, and since ℓ_p -balls are continuous spaces, there are infinitely many transformations in theory. In practice, even if we discretize the space, the number of transformations is exponentially large with respect to the input dimension. As a result, if all small transformations are allowed, (1) for non-gradient methods, we can only sample the transformations within the ℓ_p -balls; (2) for gradient methods, we can project the gradient to the ℓ_p -balls directly as described in Equations (7) and (8).

We also report the average ℓ_2 -norm of Δx for all the transformations on the test dataset. We choose ℓ_2 -norm instead of ℓ_∞ -norm because the input space and inner product used in linear approximation Equation (2) are naturally equipped with the ℓ_2 -norm. Also, the ℓ_2 -norm result can reflect the difference in ℓ_∞ -norm.

Transformation specifications. Since we test DNNs adaptively for 5 iterations, we choose the parameters for input transformations so that all the transformations evaluated in recent works are attainable within 5 iterations [6, 19, 23].

We choose $\epsilon_2 = 0.03$ and $\epsilon_\infty = 0.006$ on CIFAR10, SVHN and CIFAR100; and $\epsilon_2 = 0.32$ and $\epsilon_\infty = 0.06$ on MNIST. Because CIFAR10 and MNIST are standard datasets for adversarial learning, we use the radii from Leino et al. [19], Mueller et al. [23]. More specifically, in Leino et al. [19], Mueller et al. [23], $\epsilon_2 = 1.58$ and $\epsilon_\infty = 0.3$ for MNIST and $\epsilon_2 \approx 0.14$ and $\epsilon_\infty \approx 0.03$ for CIFAR10. We divide them by 5 to obtain the radii used in our evaluations. We choose the radii for CIFAR100 and SVHN the same as CIFAR10 because their input specifications are similar: 32×32 RGB images.

We consider 7 types of natural transformations: shift, zoom, brightness, rotation, shearing, blur, and contrast ratio as used in Gao et al. [6]. Again, parameters are selected to ensure that all these transformations are attainable within 5 iterations.

4.2 Experimental Design

RQ1. We fix randomly selected transformations for each input in the test set, and then rank the transformations based on various metrics. We consider three types of transformations separately: (i) one with only SDs, (ii) one with only natural transformations, and (iii) one with both SDs and natural transformations.

For SDs, we randomly select 14 ℓ_∞ -perturbations and 14 ℓ_2 -perturbations. For natural transformations, we generate 4 transformations for each of the seven natural transformations as in Gao et al. [6]. For mixed transformations, we combine all 28 SDs and all 28 natural transformations together as the transformation candidates.

For every set of transformations, each fitness metric produces a ranked list of transformations, where the top ones are assumed to be more likely to expose bugs in the DNN. We then compute the rank similarities between the lists. For example, given a fixed set of inputs (x_1, x_2, \dots, x_n) generated from one specific testing datum x , each metric prioritizes them to generate a ranked list. We compare the two ranked lists to study the correlation between pairs of metrics. We use the Rank Biased Overlap (RBO) to measure this similarity between a pair of ranked lists. We choose RBO as the measurement because it is well-established [36], and to the best of our knowledge, we are unaware of more suitable alternatives. The RBO score between two lists is the weighted average of overlaps between all top sublists from both lists, in which the weight takes the rank into account. The higher the score is, the more similar the two ranked lists are. One can then use RBO to measure how similar the two ranked lists are to study the correlation of the metrics.

For each input x from the testing dataset, we apply the input transformations Δx_j to get a set of transformed inputs $\{x_j\}$ with $x_j = x + \Delta x_j$. We then use a pair of metrics to rank $\{x_j\}$ and compute the RBO score of the two ranked lists. As a result, if we fix a pair of metrics, for each datum x_j , we obtain an RBO score r_j . Suppose there are n data in the test dataset (for example, $n = 26032$ for SVHN). We then have n RBO scores for each pair of metrics.

RQ2. We evaluate the metrics in the adaptive testing scenario, i.e., a repeated loop involving the mutation of inputs, the evaluation of their fitness [34], and the reception of feedback from the execution of inputs. Let us fix a metric, a DNN f , and a seed input $(x^{(0)}, y)$

from the test dataset, where 0 indicates this is the beginning of the first iteration and y is the label of $x^{(0)}$. We consider all transformations $\Delta x_j^{(0)}$ over $x^{(0)}$, so we have a set of transformed inputs $\{x_j^{(0)}\}$ generated from $x^{(0)} + \Delta x_j^{(0)}$. We then rank the transformed inputs $\{x_j^{(0)}\}$ according to the metric. Suppose $x_0^{(0)} = x^{(0)} + \Delta x_0^{(0)}$ is the best-transformed input according to the metric, we then retain $x_0^{(0)}$ as the seed input for the next iteration, i.e., $x^{(1)} = x_0^{(0)}$. In other words, we greedily choose the best transformation according to the metric for each input, and repeat this process for up to 5 iterations. In each iteration, we collect n best transformed inputs according to the metric, and use them as the seed inputs for the next iteration.

Recall that we designed metrics to detect DNN functionality bugs: inputs generated from semantics-preserving transformations and incorrectly classified. To evaluate the effectiveness of a metric, we run the DNN with the best-transformed inputs selected at the end of each iteration according to the metric, and record whether the transformed input is classified correctly with respect to the label y . Therefore, at the end of each iteration, we will get $\{c_1, \dots, c_n\}$ with $c_i \in \{0, 1\}$. $c_i = 1$ means this input is correctly classified, and $c_i = 0$ means this input is incorrectly classified. A metric that induces more incorrectly classified inputs has better bug-exposure capability.

In RQ2's experiment, we will consider three separate input transformations: natural transformations only, SDs only, and both natural transformations and SDs. The natural transformation-only scenario is similar to the evaluation in recent testing works [6, 38]. SDs only can be viewed as the adversarial attack setting [19, 21]. In particular, in the SDs-only scenario, adversarial examples created by existing attacks [10, 21] can be viewed as applications of our backward fitness scores. Because the goal of the experiment is to evaluate the bug-finding capability of different fitness, for non-gradient methods over SDs, their capability of bug-detection heavily relies on the number of sampled transformations. We, therefore, sample 140 SDs instead of 28 set in the evaluation of RQ1.

RQ3. We conduct similar experiments as those in RQ2, except that now the ground-truth labels are not available. The rationale for metamorphic testing is that metamorphic relations preserve the equivalence between inputs. Even if the ground-truth labels are unknown, if two metamorphic inputs are classified differently, at least one of the inputs is classified incorrectly, so this exposes a bug. As a result, the testing goal is to apply metamorphic relations on input and change the prediction.

We can easily adapt our metrics in the metamorphic testing scenario. Because the goal is to alter the prediction for the original inputs rather than ground-truth labels, therefore, instead of using correct labels, we use pseudo-labels predicted by the model on the original input, even though they are not necessarily correct. The goal for this testing setting is to prioritize transformed inputs that are more likely to alter the pseudo-label predictions.

The experiments are similar to RQ2's adaptive testing case. However, instead of measuring whether the input is correctly classified relative to the ground-truth label, we measure the accuracy relative to the pseudo-labels generated by the original input (without any transformations). This measurement aligns with the metamorphic

testing goal, i.e., to generate metamorphic inputs that induce different predictions. We refer to the aggregation of this measurement as pseudo-accuracy.

Statistical analysis. For all the aggregated results, we compute their average at 95% confidence intervals. The statistical analysis details can be found in Appendix D in the supplementary material.

4.3 Experimental Specifications

Baseline. We use three recent diversity-based testing works as baselines:

1. Boosting Diversity: Xie et al. [38] is our major baseline. It is built upon the assumption that if the divergence between two executions is significant, then the inputs might be classified differently. Transformed inputs with a great difference should be prioritized. As noted in Xie et al. [38], as one uses features extracted at the deeper layer of DNNs, the prioritization accuracy increases, but the execution time increases. To find the balance between these two, the standard practice is to choose the layer in the middle of the target DNN. We follow this guideline but also include a variant as a stronger baseline; we use the logit layer as the representation layer, which provides better prioritization estimation than the mid-intermediate layer.
2. NC: Ma et al. [20] monitor and gauge the intermediate neuron activities covered by current executions at various granularity levels. They profile the range of neuron outputs into k -multisections of the major function region and corner-cases regions during the training, then identify the ratio of sections covered under test-time executions. We follow the modified NC measure in Xie et al. [38] as one of our baselines.
3. ATS: Gao et al. [6] is a recently proposed metric for input selection, i.e., choosing a small yet diverse subset of inputs from a large set. We adapt it to our scenario by feeding an input and its transformed mutants to the selection algorithm one at a time and then rank the inputs based on their metric. We include this variant as another baseline.

We use the following abbreviations for the methods considered in the evaluation: **FM** stands for forward margin score (Equation (3)); **FL** stands for forward loss score (Equation (4)); **BM** stands for backward margin score (Equation (5)); **BL** stands for backward loss score (Equation (6)); **MM** stands for mixed margin score (Equation (9)); **ML** stands for mixed loss score (Equation (10)); **BD** stands for the standard tool from Xie et al. [38], **BD-F** stands for a variant that uses the logit layer to compute the divergence. **NC** stands for NC method using the layer in the middle of DNN architecture, **ATS** stands for the adapted tool from Gao et al. [6].

To summarize, our metrics (FM, FL, BM, BL, MM, ML), ATS, and BD-F only utilize the logit layer, while BD and NC use the intermediate layer neuron activations. We choose the same intermediate layer for both BD and NC. We do not include evaluations of ATS on the CIFAR100 dataset since the fault pattern computation is cubic to the number of classes, which is too slow with 100 classes.

Additional experimental setup can be found in Appendix E in the supplementary material.

5 RESULTS AND DISCUSSION

In this section, we present selected experimental results due to space limits and discussions on the results. Notice that even though we only showcase selected results in the main text, the observations presented hold for *all* experiments that we conducted, and the complete results are in the supplementary material.

5.1 RQ1

RBO baseline. A high RBO score indicates that two ranked lists are positively correlated and similar. We benchmark 3 RBO scores: (i) two same-ranked lists (denoted as *identical*); (ii) two randomly ranked lists (denoted as *random*); (iii) two opposite-ranked lists (denoted as *opposite*). Because the scores are list-length dependent, we use 10000 CIFAR10 testing inputs to benchmark these scores on lists with lengths 28 (corresponds to ℓ_p and natural transformations only) and 56 (corresponds to mixed transformations). With these benchmarks, summarized in Table 2, we can interpret the results more precisely.

Table 2: RBO score benchmark

Length	Identical	Random	Opposite
28	1.0 ± 0.0	0.518 ± 0.001	0.324 ± 0.0
56	1.0 ± 0.0	0.509 ± 0.001	0.316 ± 0.0

As a result, if the RBO score is less than 0.519 for lists of length 28 or 0.510 for lists of length 56, the two ranks are negatively correlated.

The RBO scores between different ranking methods are summarized in Table 6 in the supplementary material, and selected results are presented in Table 1.

Observations. 1. The forward loss and margin scores are always very positively correlated.

2. Diversity metrics and the loss score are quite weakly correlated when the input transformation induces small changes in the inputs. This correlation is stronger when the underlying input transformations induce large changes.

3. Forward scores and backward scores are strongly positively correlated when the underlying transformation is only SDs; however, for natural transformations, the norms induced from Δx are fairly large, and the correlations between forward and backward scores are much weaker.

Implications. 1. All the scores can be more effective in exposing functionality bugs than random prioritization. However, When applying SDs on the input, the correlation between diversity metrics and the loss change in the logit layer is quite weak. This raises concerns about their effectiveness in detecting the change in the logit layer that leads to a better chance of misclassification.

2. Both margin and loss scores can quantify how a DNN makes predictions, so their rankings of inputs to be classified incorrectly are very similar.

3. Gradient-based scores are excellent surrogates for forward scores only when the underlying transformations are SDs.

5.2 RQ2

The complete results are in Tables 7 to 9 in the supplementary material. For brevity, we discuss the results of the VGG model on CIFAR100, as the results of other models are similar. We plot the trend of accuracy in Figure 1.

Observations. In the standard testing scenario, when the underlying transformations are different, the performances of the metrics vary significantly:

1. When only SDs are presented, our backward margin (**BM**) and backward loss (**BL**) scores are by far the most effective metrics for identifying inputs that induce functionality bugs in DNNs. In particular, after the third iteration, **BM** and **BL** are close to 10 times more effective than the diversity metrics (i.e., **BD**, **BD-F**, and **NC**). In fact, diversity metrics are barely useful for finding bug-inducing inputs when only considering the SDs. Those that are highly ranked by diversity metrics rarely lead DNNs to misclassifications. Even our forward scores (i.e., **FM** and **FL**) are more effective than diversity metrics. Again, we emphasize that not accounting for SDs as an input transformation is not a valid excuse for existing diversity-based testing methods since such data points can certainly arise in the real world as inputs to DNNs.
2. When we only consider natural transformations, the forward scores produce the best results. Since the accuracy of **BD(-F)**'s is close to **FM**'s and **FL**'s, we provide a zoomed view of their averaged accuracy together with the 95% confidence interval in Table 3. The statistical analysis shows that at the third iteration, the models' accuracy is around 10-20 times lower when handling inputs identified by **FM** or **FL** compared to inputs identified by **BD(-F)**, and the margin becomes even wider at later iterations. In the meantime, the gradient-based scores are weaker than diversity-based metrics, though inputs that are highly ranked by gradient-based scores also consistently decrease models' accuracy.
3. When both SDs and natural transformations are allowed, our mixed scores are the most effective metrics.

Implications. 1. When only SDs are allowed, our backward scores are significantly more effective than diversity metrics for finding inputs that trigger bugs in DNNs. In the natural transformations-only scenario, our forward scores are the most effective in finding bug-inducing inputs. These two observations together establish the main thesis that DNN testing is a directed testing task, and the likelihood of an input inducing bugs in DNNs can be accurately measured by our directed metrics.

2. From RQ1's result, we can see that gradient surrogates are very positively correlated when input transformations are small distortions. Moreover, the linear approximation allows for the direct derivation of the optimal transformation when all SDs are allowed. This observation is consistent with our theoretical analysis and validates the application of gradient methods for SDs as in the adversarial attack case from DL literature [10, 21, 32].

3. Overall, for all input transformations, our metrics perform the best in finding inputs that cause models to misclassify. We also demonstrate the scope of each metric as presented in Section 3. As

Table 1: Similarity measures (RBO) between ranked lists according to various prioritization metrics. The first column specifies the model, dataset and accuracy on the test dataset. The second column specifies what transformations are used for the experiment. The third column norm measures the average l_2 -norm of all transformations. The rest of the columns measure the similarity between pairs of metric scores. We omit the confidence interval when it is < 0.005 .

Data, Model, Accuracy	Transformation	Norm	FM&FL	FM&BM	FL&BL	FL&BD	FL&BD-F	FL&ATS	FL&NC
SVHN ResNet-9 95.90%	SD	0.11	0.90	0.95	0.93	0.54	0.55	0.58	0.54
	Natural	8.60 ± 0.02	0.95	0.57	0.55	0.71	0.78	0.76	0.72
	Mixed	4.22 ± 0.01	0.94	0.68	0.66	0.69	0.72	0.72	0.70
CIFAR10, VGG, 91.48%	SD	0.11	0.91	0.93	0.92	0.56	0.58	0.56	0.56
	Natural	11.42 ± 0.04	0.96	0.57	0.55	0.75	0.79	0.71	0.73
	Mixed	5.67 ± 0.02	0.95	0.68	0.66	0.71	0.73	0.69	0.70

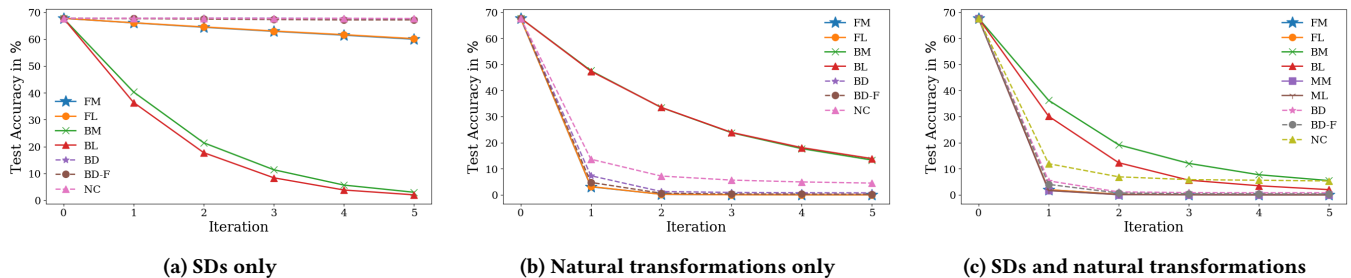


Figure 1: Accuracy change of CIFAR100 VGG in adaptive standard testing using various metrics, with different input transformations: only natural transformations, only small distortions, and both natural transformations and small distortions.

Table 3: Adaptive standard testing of each metric: the first column specifies the data, model, accuracy and input transformations. The second column specifies which metric is used for testing. The rest of the columns are the accuracy of tests prioritized by each metric during each iteration in adaptive testing. We also include the 95% confidence interval of the averaged accuracy.

Data, Model, Accuracy, Transformations	Fitness	Iter 1	Iter 2	Iter 3	Iter 4	Iter 5
CIFAR100 VGG 67.73%, Natural	FM	$3.10 \pm 0.34\%$	$0.24 \pm 0.10\%$	$0.05 \pm 0.04\%$	$0.01 \pm 0.01\%$	$0.01 \pm 0.01\%$
	FL	$3.18 \pm 0.34\%$	$0.23 \pm 0.09\%$	$0.04 \pm 0.04\%$	$0.02 \pm 0.02\%$	$0.01 \pm 0.01\%$
	BD	$7.33 \pm 0.51\%$	$1.29 \pm 0.22\%$	$0.92 \pm 0.19\%$	$0.82 \pm 0.18\%$	$0.77 \pm 0.17\%$
	BD-F	$4.77 \pm 0.42\%$	$0.63 \pm 0.16\%$	$0.33 \pm 0.11\%$	$0.28 \pm 0.10\%$	$0.23 \pm 0.09\%$

shown by our results, applying a metric outside of its scope results in a drastic degradation of its performance.

5.3 RQ3

The complete results are presented in Tables 10 to 12 in the supplementary material. We showcase the MNIST LeNet-5 model (the results for other models are similar) and plot the pseudo-accuracy changes in Figure 2.

Observations. The overall performances of the metrics are similar to the standard testing scenario: e.g., when only SDs are allowed, the diversity metrics are rather ineffective for finding bug-inducing inputs; in the natural transformations-only case, the forward metrics give the best results. We also provide a zoomed view of natural transformations-only experiment in Table 4 with the 95% confidence intervals. We still observe that our forward metrics are more

effective than the BD variants for finding inputs that trigger bugs in DNNs.

Implications. Overall, the performances of our metrics are similar to the standard testing. This implies that our directed metrics are also effective when we approach DNN functionality testing as metamorphic testing. In essence, we use a pseudo-label predicted by the model as the ground truth, and the results show that our metrics are more effective than diversity metrics in finding inputs that alter the models' prediction of the original inputs. Again, this demonstrates that the metamorphic testing of DNNs should also be treated as a directed rather than a diversity testing task.

5.4 Empirical highlights

Our evaluation reveals the following key points:

Table 4: Adaptive metamorphic testing of each metric: the first column specifies the data, model, pseudo-accuracy and input transformations. The second column specifies which metric is used for testing. The rest of the columns are the pseudo-accuracy of tests prioritized by each metric during each iteration in adaptive testing. We also include the 95% confidence interval of the averaged pseudo-accuracy.

Data, Model, Accuracy, Transformations	Fitness	Iter 1	Iter 2	Iter 3	Iter 4	Iter 5
MNIST	FM	$8.65 \pm 0.55\%$	$0.10 \pm 0.06\%$	$0.01 \pm 0.01\%$	$0.00 \pm 0.00\%$	$0.00 \pm 0.00\%$
LeNet-5	FL	$8.72 \pm 0.55\%$	$0.12 \pm 0.07\%$	$0.01 \pm 0.01\%$	$0.00 \pm 0.00\%$	$0.00 \pm 0.00\%$
100.0%,	BD	$29.37 \pm 0.89\%$	$12.71 \pm 0.65\%$	$9.81 \pm 0.58\%$	$9.06 \pm 0.56\%$	$8.43 \pm 0.54\%$
Natural	BD-F	$18.53 \pm 0.76\%$	$5.01 \pm 0.43\%$	$2.39 \pm 0.30\%$	$1.90 \pm 0.27\%$	$1.57 \pm 0.24\%$

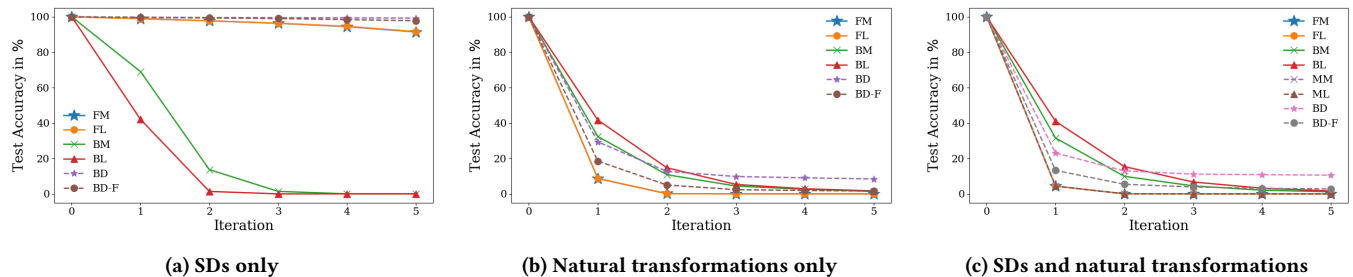


Figure 2: Pseudo-accuracy change of MNIST LeNet-5 in adaptive metamorphic testing using various metrics, with different input transformations: only natural transformations, only small distortions, and natural transformations and small distortions.

1. Diversity metrics are significantly ineffective for finding bug-inducing inputs when the input transformation is restricted to small distortions. This testing scenario has been overlooked by existing diversity-based DNN testing methods [6, 38].
2. Though both SDs and natural image transformations preserve the visual semantics, they have distinct mathematical properties and should be addressed separately for testing purposes. Applying metrics outside of their scope would result in a significant degradation in their effectiveness.
3. Regardless of the type of the underlying input transformations, our directed testing metrics are more effective in finding inputs that trigger the functionality bugs in DNNs than diversity metrics. Therefore, we substantiate the main thesis of this paper: DNN testing should be treated as a directed test task.

6 THREATS TO VALIDITY

Internal validity. Each number presented is based on the statistical analysis of at least 10,000 measurements. We justified most of the evaluation design choices except for iteration numbers. In our evaluation, we used 5 iterations to study the adaptive testing scenario. This number is not fully justified, and the parameters used in the evaluation, such as ℓ_p radii and natural input transformation parameters, depend on this iteration number. However, the 5 iteration experiment showcases examples of adaptive testing, and in each iteration, our metrics are always the best and only BD-F is relatively close to our metrics for standard testing. We re-conduct the evaluation for standard testing with iterations 3 and 8 on our metrics and BD(-F) and summarize the result in the supplementary

material. The conclusion is still the same: our metrics are superior to BD(-F) for different iteration numbers.

External validity. Our empirical results are based on 4 datasets and 3 model architectures, with various numbers of inputs, image channels (RGB v.s. grayscale), classes, and sizes. This diversity of inputs and models enhances the generalizability of our evaluations. We restrict the scope of our work to testing functionality bugs on DNNs and claim that these tasks are directed. This is because DNNs are specialized numerical programs and their mathematical semantics is simple. However, for sophisticated DL systems such as hybrid systems, which contain both DNN and traditional software, their semantics can be complicated, and testing them with designed diversity measures might be more appropriate.

7 RELATED WORK

We claim that merely increasing diversity is not the ideal framework for DNN functionality testing. However, we do not claim that diversity is useless for DL testing. It depends on our testing goal. A natural diversity issue of DL systems is fairness and bias [3, 5]: Between subgroups, DL systems contain performance discrepancies and make biased decisions towards a certain subgroup. If the tests were only from a subgroup, then potential fairness and bias issues would be concealed. Therefore, designing meaningful diversity measures can help expose and alleviate the bias and fairness issues in DL systems.

In this work, we restrict our scope to functionality bugs, i.e., inputs that are misclassified according to human perception. However, DL bugs can manifest in various forms. In Adebayo et al. [1], the authors categorize model bugs into three types: model contamination, data contamination, and test-time contamination. Model

contamination is caused by errors in the model parameters, for example, incorrectly initialized parameters; data contamination comes from defects in the training data; and test-time contamination is caused by shifts in test data. Functionality bugs can be viewed as test-time contamination: our data are transformed at test time. However, there are many more types of bugs in the DL system to be addressed and software testing techniques can be applied. For example, model contamination is often caused by API misuses, which has been studied in software engineering [14, 37].

8 CONCLUSION

In this paper, we uncover the shortcomings of diversity metrics in DNN functionality testing and advocate that it should be addressed using the directed testing framework because it is well-defined and specific. Moreover, we propose several concrete metrics to quantify the potential faultiness of inputs and carefully characterize their scopes. We find that metrics perform drastically differently across input transformations and call for careful scrutiny of these methods.

REFERENCES

- [1] Julius Adebayo, Michael Muelly, Ilaria Liccardi, and Been Kim. 2020. Debugging Tests for Model Explanations. In *Proceedings of the 34th International Conference on Neural Information Processing Systems* (Vancouver, BC, Canada) (NIPS'20). Curran Associates Inc., Red Hook, NY, USA, Article 60, 13 pages.
- [2] Marcel Böhme, Van-Thuan Pham, Manh-Dung Nguyen, and Abhik Roychoudhury. 2017. Directed Greybox Fuzzing. In *Proceedings of the 2017 ACM SIGSAC Conference on Computer and Communications Security* (Dallas, Texas, USA) (CCS '17). Association for Computing Machinery, New York, NY, USA, 2329–2344. <https://doi.org/10.1145/3133956.3134020>
- [3] Tolga Bolukbasi, Kai-Wei Chang, James Zou, Venkatesh Saligrama, and Adam Kalai. 2016. Man is to Computer Programmer as Woman is to Homemaker? Debiasing Word Embeddings. In *Proceedings of the 30th International Conference on Neural Information Processing Systems* (Barcelona, Spain) (NIPS'16). Curran Associates Inc., Red Hook, NY, USA, 4356–4364.
- [4] Songqiang Chen, Shuo Jin, and Xiaoyuan Xie. 2021. Validation on Machine Reading Comprehension Software without Annotated Labels: A Property-Based Method. In *Proceedings of the 29th ACM Joint Meeting on European Software Engineering Conference and Symposium on the Foundations of Software Engineering* (Athens, Greece) (ESEC/FSE 2021). Association for Computing Machinery, New York, NY, USA, 590–602. <https://doi.org/10.1145/3468264.3468569>
- [5] Cynthia Dwork, Moritz Hardt, Toniann Pitassi, Omer Reingold, and Richard Zemel. 2012. Fairness through awareness. In *Proceedings of the 3rd innovations in theoretical computer science conference*. 214–226.
- [6] Xinyu Gao, Yang Feng, Yining Yin, Zixi Liu, Zhenyu Chen, and Baowen Xu. 2022. Adaptive test selection for deep neural networks. In *2022 IEEE/ACM 44th International Conference on Software Engineering (ICSE)*. IEEE, 73–85.
- [7] Patrice Godefroid. 2020. Fuzzing: Hack, Art, and Science. *Commun. ACM* 63, 2 (jan 2020), 70–76. <https://doi.org/10.1145/3363824>
- [8] Ian Goodfellow, Yoshua Bengio, and Aaron Courville. 2016. *Deep Learning*. MIT Press. <http://www.deeplearningbook.org>.
- [9] Ian Goodfellow, Jean Pouget-Abadie, Mehdi Mirza, Bing Xu, David Warde-Farley, Sherjil Ozair, Aaron Courville, and Yoshua Bengio. 2014. Generative Adversarial Nets. In *Advances in Neural Information Processing Systems*, Z. Ghahramani, M. Welling, C. Cortes, N. Lawrence, and K.Q. Weinberger (Eds.), Vol. 27. Curran Associates, Inc. https://proceedings.neurips.cc/paper_files/paper/2014/file/5ca3e9b122f61f8f06494c97b1afcc3-Paper.pdf
- [10] Ian J. Goodfellow, Jonathon Shlens, and Christian Szegedy. 2015. Explaining and Harnessing Adversarial Examples. In *3rd International Conference on Learning Representations, ICLR 2015, San Diego, CA, USA, May 7-9, 2015, Conference Track Proceedings*, Yoshua Bengio and Yann LeCun (Eds.). <http://arxiv.org/abs/1412.6572>
- [11] Fabrice Harel-Canada, Lingxiao Wang, Muhammad Ali Gulzar, Quanquan Gu, and Miryung Kim. 2020. Is Neuron Coverage a Meaningful Measure for Testing Deep Neural Networks?. In *Proceedings of the 28th ACM Joint Meeting on European Software Engineering Conference and Symposium on the Foundations of Software Engineering* (Virtual Event, USA) (ESEC/FSE 2020). Association for Computing Machinery, New York, NY, USA, 851–862. <https://doi.org/10.1145/3368089.3409754>
- [12] Kaiming He, Xiangyu Zhang, Shaoqing Ren, and Jian Sun. 2016. Deep Residual Learning for Image Recognition. In *2016 IEEE Conference on Computer Vision and Pattern Recognition (CVPR)*. 770–778. <https://doi.org/10.1109/CVPR.2016.90>
- [13] Dae R. Jeong, Kyungtae Kim, Basavesh Shivakumar, Byoungyoung Lee, and Insik Shin. 2019. Razer: Finding Kernel Race Bugs through Fuzzing. In *2019 IEEE Symposium on Security and Privacy (SP)*. 754–768. <https://doi.org/10.1109/SP.2019.00017>
- [14] Hong Jin Kang and David Lo. 2022. Active Learning of Discriminative Subgraph Patterns for API Misuse Detection. *IEEE Transactions on Software Engineering* 48, 8 (2022), 2761–2783. <https://doi.org/10.1109/TSE.2021.3069978>
- [15] Alex Krizhevsky, Geoffrey Hinton, et al. 2009. Learning multiple layers of features from tiny images. (2009).
- [16] Alex Krizhevsky, Ilya Sutskever, and Geoffrey E. Hinton. 2017. ImageNet Classification with Deep Convolutional Neural Networks. *Commun. ACM* 60, 6 (may 2017), 84–90. <https://doi.org/10.1145/3065386>
- [17] Yann LeCun, Léon Bottou, Yoshua Bengio, and Patrick Haffner. 1998. Gradient-based learning applied to document recognition. *Proc. IEEE* 86, 11 (1998), 2278–2324.
- [18] Yann LeCun and Corinna Cortes. 2010. MNIST handwritten digit database. <http://yann.lecun.com/exdb/mnist/>. (2010). <http://yann.lecun.com/exdb/mnist/>
- [19] Klas Leino, Zifan Wang, and Matt Fredrikson. 2021. Globally-Robust Neural Networks. In *International Conference on Machine Learning (ICML)*.
- [20] Lei Ma, Felix Juefei-Xu, Fuyuan Zhang, Jiyuan Sun, Minhui Xue, Bo Li, Chunyang Chen, Ting Su, Li Li, Yang Liu, Jianjun Zhao, and Yadong Wang. 2018. DeepGauge: Multi-Granularity Testing Criteria for Deep Learning Systems. In *Proceedings of the 33rd ACM/IEEE International Conference on Automated Software Engineering* (Montpellier, France) (ASE '18). Association for Computing Machinery, New York, NY, USA, 120–131. <https://doi.org/10.1145/3238147.3238202>
- [21] Aleksander Madry, Aleksandar Makelov, Ludwig Schmidt, Dimitris Tsipras, and Adrian Vladu. 2018. Towards Deep Learning Models Resistant to Adversarial Attacks. In *International Conference on Learning Representations*.
- [22] Tomas Mikolov, Ilya Sutskever, Kai Chen, Greg Corrado, and Jeffrey Dean. 2013. Distributed Representations of Words and Phrases and Their Compositionality. In *Proceedings of the 26th International Conference on Neural Information Processing Systems - Volume 2* (Lake Tahoe, Nevada) (NIPS'13). Curran Associates Inc., Red Hook, NY, USA, 3111–3119.
- [23] Mark Niklas Mueller, Franziska Eckert, Marc Fischer, and Martin Vechev. 2023. Certified Training: Small Boxes are All You Need. In *The Eleventh International Conference on Learning Representations*.
- [24] Yuval Netzer, Tao Wang, Adam Coates, Alessandro Bissacco, Bo Wu, and Andrew Y. Ng. 2011. Reading Digits in Natural Images with Unsupervised Feature Learning. In *NIPS Workshop on Deep Learning and Unsupervised Feature Learning 2011*. http://ufl.stanford.edu/housenumbers/nips2011_housenumbers.pdf
- [25] S. Pavlitskaya, S. Yikmis, and J. Zollner. 2022. Is Neuron Coverage Needed to Make Person Detection More Robust?. In *2022 IEEE/CVF Conference on Computer Vision and Pattern Recognition Workshops (CVPRW)*. IEEE Computer Society, Los Alamitos, CA, USA, 2888–2896. <https://doi.org/10.1109/CVPRW56347.2022.00326>
- [26] Kexin Pei, Yinzhi Cao, Junfeng Yang, and Suman Jana. 2019. DeepXplore: Automated Whitebox Testing of Deep Learning Systems. *Commun. ACM* 62, 11 (oct 2019), 137–145. <https://doi.org/10.1145/3361566>
- [27] Robin Rombach, Andreas Blattmann, Dominik Lorenz, Patrick Esser, and Björn Ommer. 2022. High-resolution image synthesis with latent diffusion models. In *Proceedings of the IEEE/CVF Conference on Computer Vision and Pattern Recognition*. 10684–10695.
- [28] W. Rudin. 1986. *Principles of Mathematical Analysis*. McGraw - Hill Book Co. <https://books.google.com/books?id=frdNAQAACAAJ>
- [29] Skipper Seabold and Josef Perktold. 2010. statsmodels: Econometric and statistical modeling with python. In *9th Python in Science Conference*.
- [30] Connor Shorten and Taghi M Khoshgoufar. 2019. A survey on image data augmentation for deep learning. *Journal of big data* 6, 1 (2019), 1–48.
- [31] Karen Simonyan and Andrew Zisserman. 2015. Very Deep Convolutional Networks for Large-Scale Image Recognition. arXiv:1409.1556 [cs.CV]
- [32] Christian Szegedy, Wojciech Zaremba, Ilya Sutskever, Joan Bruna, Dumitru Erhan, Ian J. Goodfellow, and Rob Fergus. 2014. Intriguing properties of neural networks. In *2nd International Conference on Learning Representations, ICLR 2014, Banff, AB, Canada, April 14-16, 2014, Conference Track Proceedings*, Yoshua Bengio and Yann LeCun (Eds.). <http://arxiv.org/abs/1312.6199>
- [33] Pauli Virtanen, Ralf Gommers, Travis E. Oliphant, Matt Haberland, Tyler Reddy, David Cournapeau, Evgeni Burovski, Pearu Peterson, Warren Weckesser, Jonathan Bright, Stéfan J. van der Walt, Matthew Brett, Joshua Wilson, K. Jarrod Millman, Nikolay Mayorov, Andrew R. J. Nelson, Eric Jones, Robert Kern, Eric Larson, C. J. Carey, Ilhan Polat, Yu Feng, Eric W. Moore, Jake VanderPlas, Denis Laxalde, Josef Perktold, Robert Cimrman, Ian Henriksen, E. A. Quintero, Charles R. Harris, Anne M. Archibald, António H. Ribeiro, Fabian Pedregosa, Paul van Mulbregt, and SciPy 1.0 Contributors. 2020. SciPy 1.0: Fundamental Algorithms for Scientific Computing in Python. *Nature Methods* 17 (2020), 261–272. <https://doi.org/10.1038/s41592-019-0686-2>
- [34] Zi Wang, Ben Liblit, and Thomas W. Reps. 2020. TOFU: Target-Oriented FUZZer. *CoRR abs/2004.14375* (2020). arXiv:2004.14375 <https://arxiv.org/abs/2004.14375>

- [35] Larry Wasserman. 2010. *All of statistics : a concise course in statistical inference*. Springer, New York. http://www.amazon.de/All-Statistics-Statistical-Inference-Springer/dp/1441923225/ref=sr_1_2?ie=UTF8&qid=1356099149&sr=8-2
- [36] William Webber, Alistair Moffat, and Justin Zobel. 2010. A Similarity Measure for Indefinite Rankings. *ACM Trans. Inf. Syst.* 28, 4, Article 20 (nov 2010), 38 pages. <https://doi.org/10.1145/1852102.1852106>
- [37] Ming Wen, Yepang Liu, Rongxin Wu, Xuan Xie, Shing-Chi Cheung, and Zhendong Su. 2019. Exposing Library API Misuses Via Mutation Analysis. In *2019 IEEE/ACM 41st International Conference on Software Engineering (ICSE)*. 866–877. <https://doi.org/10.1109/ICSE.2019.00093>
- [38] Xiaoyuan Xie, Pengbo Yin, and Songqiang Chen. 2023. Boosting the Revealing of Detected Violations in Deep Learning Testing: A Diversity-Guided Method. In *Proceedings of the 37th IEEE/ACM International Conference on Automated Software Engineering (Rochester, MI, USA) (ASE '22)*. Association for Computing Machinery, New York, NY, USA, Article 17, 13 pages. <https://doi.org/10.1145/3551349.3556919>
- [39] Michal Zalewski. 2022. american fuzzy lop. <https://lcamtuf.coredump.cx/afl/>.

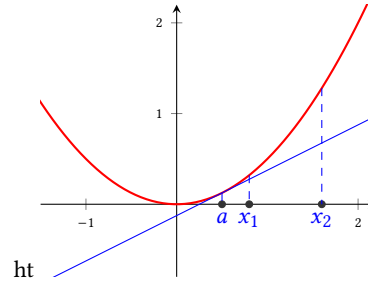


Figure 3: An illustration of linear approximation of $f(x) = 0.5 * x^2$ (red curve) at $a = 0.5$. One can use the gradient of f to construct the linear approximation as in the blue line, which is close to f when x_1 is close to a , but distant when x_2 is far from a .

A A LINEAR APPROXIMATION ILLUSTRATION

B GRADIENT METHODS RUNNING-TIME ANALYSIS

Suppose there are N transformations for an input, a forward execution takes F time, a backward gradient execution takes B time, which is usually similar to F , and the inner-product computation takes I time. To compute the forward fitness score, we need N forward executions, which take NF time. To compute the backward fitness score, we need 1 forward execution to compute $f(x)$ and 1 backward execution to compute the gradient $Df(x)$, and then N inner-product computations to compute $(\Delta x)^T D(f)(x)$, which is usually very cheap compared to DNN executions. Brought together, the backward fitness score takes $F + B + NI$ time to finish.

C PROOF OF PROPOSITION 3.1

PROOF. Let us fix an input a . The goal is to maximize the linear approximation of a function $f(x)$ at a within the ℓ_p -balls with radii ϵ centered at a .

Because the balls are centered at a , each point in the ball can be expressed as $a + \Delta x$ with $\|\Delta x\|_p \leq \epsilon$, and the linear approximation at the point is:

$$f(a) + (\Delta x)^T Df(a).$$

Let us use h to denote $Df(a)$. To maximize this term, we only need to maximize $(\Delta x)^T h$.

If $\|\Delta x\|_2 \leq \epsilon$, because $(\Delta x)^T h = \|\Delta x\|_2 \|h\|_2 \cos \theta$, where θ is the angle between the two vectors Δx and $Df(a)$, we know that $\|\Delta x\|_2 \leq \epsilon$ and $\cos \theta \leq 1$, then $(\Delta x)^T Df(a) \leq \epsilon \|h\|_2$. On the other hand, if $\Delta x = \frac{h}{\|h\|_2} \epsilon$, then $(\Delta x)^T h = \frac{h^T h}{\|h\|_2} \epsilon = \epsilon \|h\|_2$. This shows that Equation (7) is the optimal solution to the linear approximation in the ℓ_2 -ball.

Notice that in above proof, we only need $(\Delta x)^T h \leq \|\Delta x\|_2 \|h\|_2$, which can be directly derived from the Cauchy–Schwarz inequality. If we generalize the Cauchy–Schwarz inequality to Hölder’s inequality, we can immediately get the result for the ℓ_∞ -case.

More formally, if $\|\Delta x\|_\infty \leq \epsilon$, then by Hölder’s inequality, $(\Delta x)^T h \leq \|\Delta x\|_\infty \|h\|_1 \leq \epsilon \|h\|_1$. On the other hand, if $\Delta x = \epsilon * \text{sign}(h)$, then $(\Delta x)^T h = \epsilon * \text{sign}(h)h = \epsilon \sum |h_i| = \epsilon \|h\|_1$. This

shows that Equation (8) is the optimal solution to the linear approximation in the ℓ_∞ -ball.

□

D STATISTICAL DATA ANALYSIS

In RQ1, for each single datum, we measure the RBO score, a continuous value between $[0, 1]$. For RQ2 and RQ3, for every datum, we measure the accuracy, a binary value from $\{0, 1\}$, which stands for wrong and correct classification, respectively. As a result, for RQ1, we collect a set of RBO scores $\{r_1, \dots, r_n\}$, where n is the number of testing inputs and $r_i \in [0, 1]$; and for RQ2 and RQ3, in each iteration for each metric, we collect a set of accuracy values $\{c_1, \dots, c_n\}$, where $c_i \in \{0, 1\}$.

We conduct statistical data analysis on two types of random variables: continuous-valued and binary-valued. Because each statistic is from thousands of measurements, i.e., each datum in the testing dataset produces a measurement, we use the normal distribution to model the data distribution due to central limit theorem [35] and the Scipy.stats [33] and statsmodels [29] packages to compute the confidence interval.

E ADDITIONAL EXPERIMENTAL SPECIFICATIONS

Table 5: Datasets and Models

Dataset	Description	Model	Layer	# Parameters
MNIST	70000 28×28 grayscale images	LeNet-1	5	3246
		LeNet-5	7	61706
SVHN	99289 32×32 RGB images	VGG-16	21	14990922
		ResNet-9	9	2274880
CIFAR10	60000 32×32 RGB images	VGG-16	21	14990922
		ResNet-18	18	11173962
CIFAR100	60000 32×32 RGB images	VGG-16	21	15037092
		ResNet-18	18	11220132

Server specification. All the experiments are run on a workstation with forty-eight Intel® Xeon® Silver 4214 CPUs running at 2.20GHz, and 258 GB of memory, and eight Nvidia GeForce RTX 2080 Ti GPUs. Each GPU has 4352 CUDA cores and 11 GB of GDDR6 memory.

Training specifications. We use batch size 500, the SGD optimizer with learning rate 0.1, momentum 0.9, decay $5e^{-4}$ to train the networks, and each model is trained for 100 epochs. To ensure reproducibility, we also explicitly specify seeds for all random functions.

F DIFFERENT ITERATION NUMBERS

We rerun the experiments for RQ2 on our forward metrics and BD(-F), as if the iterations were 3 or 8. Therefore, we also adjust the parameters for the input transformations accordingly. For example, if for the 5 iterations, the shift step is 0.3, then for the 3 iteration experiment, we adjust the step to 0.5 and for the 8 iteration experiment, we adjust the step to 0.1875. The rationale is that we want to make sure the total step size for all experiments are the same, i.e., $0.3 \times 5 = 0.5 \times 3 = 0.1875 \times 8$. The results are presented in Tables 13 and 14. Notice that the result is consistent with our 5-iteration experiments.

Table 6: Similarity measures (RBO) between ranked lists according to various prioritization metrics. The first column specifies the model, dataset and accuracy on the test dataset. The second column specifies what transformations are used for the experiment. The third column norm measures the average ℓ_2 -norm of all transformations. The rest of the columns measure the similarity between pairs of metric scores. We omit the confidence interval when it is < 0.005 .

Data Model, Accuracy	Transformation	Norm	FM&FL	FM&BM	FL&BL	FL&BD	FL&BD-F	FL&ATS	FL&NC
MNIST	SD	0.65	0.89	0.95	0.94	0.57	0.57	0.74	0.57
LeNet-1 97.32%	Natural	2.68 ± 0.02	0.94	0.84	0.75	0.76	0.77	0.81	0.67
	Mixed	1.77 ± 0.01	0.93	0.87	0.82	0.71	0.72	0.77	0.66
MNIST	SD	0.65	0.89	0.96	0.94	0.57	0.59	0.67	0.56
LeNet-5 99.01%	Natural	2.68 ± 0.02	0.95	0.84	0.76	0.77	0.79	0.81	0.66
	Mixed	1.77 ± 0.01	0.93	0.88	0.83	0.72	0.74	0.76	0.64
SVHN	SD	0.11	0.90	0.95	0.93	0.54	0.55	0.58	0.54
ResNet-9 95.90%	Natural	8.60 ± 0.02	0.95	0.57	0.55	0.71	0.78	0.76	0.72
	Mixed	4.22 ± 0.01	0.94	0.68	0.66	0.69	0.72	0.72	0.70
SVHN	SD	0.11	0.88	0.95	0.94	0.56	0.57	0.56	0.56
VGG 95.19%	Natural	8.60 ± 0.02	0.94	0.61	0.60	0.71	0.76	0.70	0.70
	Mixed	4.22 ± 0.01	0.92	0.72	0.70	0.67	0.70	0.67	0.67
CIFAR10, ResNet-18, 92.29%	SD	0.11	0.90	0.90	0.90	0.56	0.57	0.58	0.56
	Natural	11.42 ± 0.04	0.95	0.57	0.56	0.76	0.80	0.76	0.71
	Mixed	5.67 ± 0.02	0.95	0.68	0.66	0.73	0.75	0.73	0.70
CIFAR10, VGG, 91.48%	SD	0.11	0.91	0.93	0.92	0.56	0.58	0.56	0.56
	Natural	11.42 ± 0.04	0.96	0.57	0.55	0.75	0.79	0.71	0.73
	Mixed	5.67 ± 0.02	0.95	0.68	0.66	0.71	0.73	0.69	0.70
CIFAR100 ResNet-18 70.45%	SD	0.11	0.85	0.88	0.88	0.55	0.57	–	0.55
	Natural	11.69 ± 0.04	0.89	0.59	0.56	0.76	0.79	–	0.75
	Mixed	5.80 ± 0.03	0.89	0.69	0.66	0.73	0.75	–	0.73
CIFAR100 VGG 67.73%	SD	0.11	0.91	0.90	0.90	0.56	0.58	–	0.56
	Natural	11.69 ± 0.04	0.95	0.59	0.57	0.75	0.78	–	0.72
	Mixed	5.80 ± 0.03	0.95	0.70	0.67	0.72	0.73	–	0.70

Table 7: Adaptive standard testing of each metric: the first column specifies the data, model, clean accuracy, and underlying data transformations. The second column specifies which metric is used for testing. The rest of the columns are the accuracy of tests prioritized by each metric during each iteration in adaptive testing. We include the confidence interval when the result from diversity metrics is close to our best directed-metric result.

Data, Model, Accuracy, Transformations	Fitness	Iter 1	Iter 2	Iter 3	Iter 4	Iter 5
MNIST LeNet-1 97.32% Natural	FM	6.66%	0.49%	0.36%	0.36%	0.36%
	FL	10.20%	0.11%	0.07%	0.07%	0.07%
	BM	28.46%	10.27%	4.51%	2.58%	1.87%
	BL	41.42%	16.36%	7.58%	4.23%	2.54%
	BD	25.5%	16.2%	14.27%	13.01%	12.30%
	BD-F	18.05%	7.04%	4.69%	3.88%	3.49%
	ATS	29.56%	19.86%	17.31%	16.42%	16.24%
	NC	78.83%	76.90%	74.52%	72.64%	71.71%
MNIST LeNet-5 99.01% Natural	FM	4.93%	0.08%	0.01%	0.0%	0.0%
	FL	4.97%	0.1%	0.01%	0.0%	0.0%
	BM	28.63%	10.13%	4.33%	2.04%	1.37%
	BL	37.63%	13.27%	5.19%	2.43%	1.43%
	BD	25.43%	11.51%	9.99%	9.18%	9.13%
	BD-F	14.22%	4.06%	2.52%	2.11%	1.88%
	ATS	27.74%	19.97%	17.6%	16.61%	16.33%
	NC	80.51%	79.72%	78.83%	78.09%	77.66%
SVHN ResNet-9 95.90% Natural	FM	20.71%	1.95%	0.38%	0.29%	0.26%
	FL	20.91%	2.19%	0.47%	0.33%	0.29%
	BM	80.72%	57.59%	41.37%	31.87%	24.21%
	BL	81.29%	59.57%	43.64%	33.72%	25.60%
	BD	36.16%	13.98%	10.23%	9.82%	9.73%
	BD-F	24.93%	4.58%	1.77%	1.29%	1.09%
	ATS	30.39%	19.52%	17.06%	15.84%	15.47%
	NC	39.75%	15.17%	10.51%	9.94%	9.92%
SVHN VGG 95.19% Natural	FM	18.12%	4.28%	2.79%	2.34%	2.05%
	FL	18.15%	4.79%	3.33%	2.83%	2.50%
	BM	74.77%	54.19%	38.43%	30.36%	24.23%
	BL	75.52%	52.11%	37.04%	28.30%	21.66%
	BD	28.96%	18.57%	19.45%	19.52%	19.51%
	BD-F	20.64%	6.53%	4.71%	4.11%	3.71%
	ATS	33.05%	22.69%	19.88%	18.70%	17.91%
	NC	33.80%	23.40%	21.59%	20.95%	20.70%

Table (Continued)

CIFAR10, ResNet-18, 92.29% Natural	FM	10.78%	1.02%	0.42%	0.25%	0.20%
	FL	10.92%	1.17%	0.47%	0.27%	0.20%
	BM	71.45%	55.24%	41.98%	33.90%	27.93%
	BL	78.63%	63.79%	50.71%	41.79%	35.42%
	BD	24.41%	13.38%	11.75%	11.50%	11.45%
	BD-F	17.00%	4.56%	2.41%	1.74%	1.57%
	ATS	29.49%	21.46%	19.92%	18.61%	17.95%
	NC	40.41%	30.49%	26.20%	24.53%	23.50%
CIFAR10 VGG 91.48% Natural	FM	8.43%	1.26%	0.56%	0.44%	0.32%
	FL	8.46%	1.34%	0.68%	0.56%	0.47%
	BM	74.82%	59.75%	47.60%	39.35%	32.23%
	BL	74.96%	60.4%	48.92%	40.27%	33.51%
	BD	16.85%	9.71%	9.53%	9.35%	9.34%
	BD-F	11.56%	3.23%	2.05%	1.61%	1.28%
	ATS	29.49%	21.46%	19.92%	18.61%	17.95%
	NC	24.32%	15.14%	12.82%	11.82%	11.28%
CIFAR100 ResNet-18 70.45% Natural	FM	3.32%	0.27%	0.10 ± 0.06%	0.03 ± 0.03%	0.02 ± 0.02%
	FL	3.88%	0.29%	0.10 ± 0.06%	0.06 ± 0.05%	0.05 ± 0.04%
	BM	50.19%	35.72%	26.21%	19.65%	14.97%
	BL	50.03%	35.84%	26.46%	19.81%	15.46%
	BD	10.54%	1.67%	0.98%	1.01%	0.96%
	BD-F	5.69%	0.62%	0.36 ± 0.11%	0.20 ± 0.09%	0.18 ± 0.08%
	NC	12.95%	3.88%	2.37%	1.94%	1.80%
CIFAR100, VGG 67.73% Natural	FM	3.10%	0.24%	0.05%	0.01%	0.01%
	FL	3.18%	0.23%	0.04%	0.02%	0.01%
	BM	47.61%	33.49%	23.82%	17.72%	13.34%
	BL	47.39%	33.54%	23.95%	18.11%	13.89%
	BD	7.33%	1.29%	0.92%	0.82%	0.77%
	BD-F	4.77%	0.63%	0.33%	0.28%	0.23%
	NC	13.66%	7.21%	5.66%	4.95%	4.51%
CIFAR100, VGG 67.73% Natural	FM	3.10%	0.24%	0.05%	0.01%	0.01%
	FL	3.18%	0.23%	0.04%	0.02%	0.01%
	BM	47.61%	33.49%	23.82%	17.72%	13.34%
	BL	47.39%	33.54%	23.95%	18.11%	13.89%
	BD	7.33%	1.29%	0.92%	0.82%	0.77%
	BD-F	4.77%	0.63%	0.33%	0.28%	0.23%
	NC	13.66%	7.21%	5.66%	4.95%	4.51%

Table 8: Adaptive standard testing of each metric: the first column specifies the data, model, clean accuracy, and underlying data transformations. The second column specifies which metric is used for testing. The rest of the columns are the accuracy of tests prioritized by each metric during each iteration in adaptive testing. We include the confidence interval when the result from diversity metrics is close to our best directed-metric result.

Data Model Accuracy Transformations	Fitness	Iter 1	Iter 2	Iter 3	Iter 4	Iter 5
MNIST LeNet-1 97.32% SD	FM	96.35%	94.93%	92.89%	90.20%	86.62%
	FL	96.38%	95.06%	93.02%	90.37%	86.98%
	BM	70.36%	15.45%	2.47%	0.28%	0.03%
	BL	33.02%	0.65%	0.0%	0.0%	0.0%
	BD	97.32%	97.27%	97.14%	97.02%	96.90%
	BD-F	97.21%	97.19%	97.08%	96.93%	96.67%
	ATS	97.19%	96.61%	95.67%	94.62%	93.0%
	NC	97.27%	97.24%	97.26%	97.19%	97.26%
MNIST LeNet-5 99.01% SD	FM	98.32%	97.42%	96.14%	94.36%	91.74%
	FL	98.34%	97.41%	96.17%	94.43%	91.89%
	BM	69.15%	13.62%	1.51%	0.05%	0.0%
	BL	42.06%	1.39%	0.01%	0.0%	0.0%
	BD	98.89%	98.84%	98.75%	98.65%	98.62%
	BD-F	98.91%	98.77%	98.55%	98.21%	97.66%
	ATS	98.90%	98.50%	97.90%	96.83%	95.38%
	NC	98.89%	98.89%	98.85%	98.82%	98.84%
SVHN ResNet-9 95.90% SD	FM	95.61%	95.31%	95.00%	94.69%	94.30%
	FL	95.62%	95.32%	95.03%	94.74%	94.34%
	BM	89.23%	77.71%	63.88%	50.65%	39.01%
	BL	86.45%	71.06%	54.72%	40.96%	29.85%
	BD	95.88%	95.87%	95.87%	95.89%	95.87%
	BD-F	95.87%	95.86%	95.83%	95.82%	95.77%
	ATS	95.89%	95.81%	95.77%	95.70%	95.63%
	NC	95.87%	95.91%	95.90%	95.89%	95.89%
SVHN VGG 95.19% SD	FM	94.93%	94.57%	94.21%	93.86%	93.56%
	FL	94.94%	94.58%	94.23%	93.87%	93.57%
	BM	85.38%	73.49%	62.97%	53.38%	44.24%
	BL	84.88%	71.77%	59.85%	49.03%	39.40%
	BD	95.18%	95.16%	95.15%	95.08%	95.06%
	BD-F	95.18%	95.17%	95.15%	95.09%	95.01%
	ATS	95.21%	95.17%	94.95%	94.91%	94.87%
	NC	95.17%	95.16%	95.12%	95.08%	95.03%

Table (Continued)

CIFAR10 ResNet-18 92.29% SD	FM	91.40%	90.55%	89.31%	88.24%	87.11%
	FL	91.44%	90.59%	89.33%	88.33%	87.26%
	BM	67.76%	42.21%	26.08%	15.82%	9.53%
	BL	64.75%	37.16%	20.80%	10.94%	6.08%
	BD	92.31%	92.35%	92.20%	92.18%	92.12%
	BD-F	92.27%	92.22%	92.20%	91.98%	91.90%
	ATS	92.27%	92.32%	91.70%	91.51%	91.23%
	NC	92.25%	92.21%	92.26%	92.18%	92.20%
CIFAR10 VGG 91.48% SD	FM	90.90%	90.05%	89.40%	88.61%	87.76%
	FL	90.90%	90.05%	89.43%	88.63%	87.74%
	BM	70.45%	50.69%	36.69%	26.54%	18.94%
	BL	69.54%	48.64%	34.26%	24.22%	16.55%
	BD	91.46%	91.61%	91.50%	91.30%	91.25%
	BD-F	91.47%	91.51%	91.40%	91.18%	90.93%
	ATS	91.46%	91.37%	91.13%	91.31%	91.00%
	NC	91.52%	91.52%	91.55%	91.53%	91.35%
CIFAR100 ResNet-18 70.45% SD	FM	68.18%	65.77%	63.47%	61.30%	59.09%
	FL	68.58%	66.53%	64.52%	62.60%	60.62%
	BM	36.73%	13.77%	4.40%	1.51%	0.57%
	BL	33.07%	11.27%	3.53%	1.22%	0.42%
	BD	70.42%	70.33%	70.39%	70.42%	70.25%
	BD-F	70.30%	70.08%	69.80%	69.60%	69.04%
	NC	70.51%	70.51%	70.29%	70.17%	70.14%
CIFAR100 VGG 67.73% SD	FM	66.05%	64.42%	62.90%	61.48%	59.97%
	FL	66.09%	64.54%	63.01%	61.65%	60.18%
	BM	40.32%	21.43%	11.39%	5.69%	3.02%
	BL	36.42%	17.75%	8.39%	3.86%	2.06%
	BD	67.73%	67.84%	67.78%	67.68%	67.60%
	BD-F	67.64%	67.45%	67.30%	67.15%	67.16%
	NC	67.75%	67.78%	67.67%	67.73%	67.67%

Table 9: Adaptive standard testing of each metric: the first column specifies the data, model, clean accuracy, and underlying data transformations. The second column specifies which metric is used for testing. The rest of the columns are the accuracy of tests prioritized by each metric during each iteration in adaptive testing. We include the confidence interval when the result from diversity metrics is close to our best directed-metric result. Notice that we do not include the result of NC for SVHN because it is too slow to finish the iterations (over 30 hours).

Data Model Accuracy Transformations	Fitness	Iter 1	Iter 2	Iter 3	Iter 4	Iter 5
MNIST LeNet-1 97.32% Mixed	FM	10.06%	0.37%	0.0%	0.0%	0.0%
	FL	10.44%	0.39%	0.02%	0.0%	0.0%
	BM	35.94%	12.81%	5.79%	3.28%	2.16%
	BL	49.18%	20.23%	10.11%	5.94%	3.30%
	MM	10.05%	0.26%	0.01%	0.0%	0.0%
	ML	10.38%	0.16%	0.0%	0.0%	0.0%
	BD	27.68%	16.50%	14.72%	14.08%	12.57%
	BD-F	21.09%	7.60%	4.74%	3.67%	3.43%
	ATS	34.41%	22.92%	19.78%	17.56%	16.70%
MNIST LeNet-5 99.01% Mixed	NC	78.52%	78.38%	78.10%	78.02%	78.07%
	FM	8.47%	0.07%	0.0%	0.0%	0.0%
	FL	8.56%	0.09%	0.0%	0.0%	0.0%
	BM	40.23%	12.43%	5.12%	2.17%	1.27%
	BL	48.78%	18.41%	6.98%	3.67%	1.77%
	MM	8.47%	0.07%	0.0%	0.0%	0.0%
	ML	8.52%	0.05%	0.0%	0.0%	0.0%
	BD	36.45%	9.26%	8.99%	8.92%	8.85%
	BD-F	18.60%	4.88%	2.94%	2.57%	2.26%
ATS	31.08%	21.58%	19.01%	18.17%	16.82%	
SVHN ResNet-9 95.90% Mixed	NC	88.81%	87.93%	87.39%	87.13%	86.95%
	FM	15.04%	2.65%	0.56%	0.04%	0.0%
	FL	15.31%	2.89%	0.68%	0.08%	0.02%
	BM	79.26%	57.53%	38.51%	26.85%	18.97%
	BL	76.82%	51.28%	31.30%	18.42%	11.41%
	MM	14.58%	1.62%	0.12%	0.02%	0.0%
	ML	14.54%	1.66%	0.13%	0.0%	0.0%
	BD	34.93%	17.16%	11.24%	10.20%	10.17%
	BD-F	18.53%	5.16%	2.05%	1.10%	0.86%
ATS	30.88%	19.96%	17.83%	16.81%	16.29%	

Table (Continued)

SVHN VGG 95.19% Mixed	FM	16.29%	4.93%	2.70%	2.14%	1.85%
	FL	16.35%	5.42%	3.24%	2.57%	2.23%
	BM	74.12%	52.57%	35.21%	23.53%	15.73%
	BL	75.02%	53.71%	35.45%	22.37%	13.86%
	MM	16.76%	1.33%	0.10%	0.00%	0.00%
	ML	16.63%	1.36%	0.10%	0.01%	0.00%
	BD	27.64%	19.58%	19.22%	19.49%	19.56%
	BD-F	18.75%	7.21%	4.86%	4.08%	3.58%
	ATS	33.97%	22.78%	19.80%	18.49%	17.46%
CIFAR10 ResNet-18 92.29% Mixed	FM	8.01%	0.99%	0.29%	0.16%	0.07%
	FL	8.14%	1.06%	0.33%	0.17%	0.08%
	BM	58.85%	33.99%	21.55%	14.90%	10.88%
	BL	54.01%	25.60%	12.16%	6.22%	3.39%
	MM	6.79%	0.30%	0.05%	0.01%	0.00%
	ML	6.69%	0.30%	0.05%	0.00%	0.00%
	BD	22.02%	12.73%	12.15%	12.20%	12.36%
	BD-F	13.91%	4.13%	2.37%	1.77%	1.41%
	ATS	31.02%	20.91%	18.58%	18.06%	17.81%
CIFAR10 VGG 91.48% Mixed	NC	35.87%	31.98%	31.20%	31.04%	30.86%
	FM	6.17%	1.40%	0.91%	0.70%	0.55%
	FL	6.22%	1.52%	1.05%	0.88%	0.79%
	BM	64.06%	43.81%	30.27%	21.07%	14.81%
	BL	63.13%	40.55%	25.21%	15.81%	9.46%
	MM	4.86%	0.48%	0.11%	0.01%	0.00%
	ML	4.84%	0.50%	0.11%	0.02%	0.00%
	BD	15.90%	9.75%	9.59%	9.61%	9.61%
	BD-F	9.38%	3.38%	2.60%	2.27%	2.02%
CIFAR100 ResNet-18 70.45% Mixed	ATS	30.83%	22.69%	20.51%	19.59%	20.01%
	NC	20.74%	14.07%	13.07%	12.73%	12.58%
	FM	2.17%	0.22%	0.03%	0.00%	0.00%
	FL	2.46%	0.28%	0.08%	0.04%	0.01%
	BM	28.91%	15.24%	10.62%	7.69%	5.19%
	BL	23.54%	6.16%	2.26%	1.13%	0.87%
	MM	1.56%	0.01%	0.00%	0.00%	0.00%
	ML	1.67%	0.01%	0.00%	0.00%	0.00%
	BD	7.84%	1.76%	1.15%	1.12%	1.07%
BD-F	4.50%	0.72%	0.40%	0.30%	0.27%	
NC	10.06%	3.90%	3.01%	2.68%	2.65%	

Table (Continued)

CIFAR100 VGG 67.73% Mixed	FM	1.94%	0.19%	0.05%	0.01%	0.01%
	FL	1.97%	0.22%	0.05%	0.02%	0.01%
	BM	36.23%	19.18%	12.05%	7.70%	5.46%
	BL	30.14%	12.30%	5.62%	3.48%	1.99%
	MM	1.63%	0.07%	0.02%	0.01%	0.00%
	ML	1.66%	0.09%	0.02%	0.00%	0.00%
	BD	5.35%	1.11%	0.85%	0.79%	0.80%
	BD-F	4.00%	0.70%	0.43%	0.38%	0.35%
	NC	11.94%	6.90%	5.83%	5.59%	5.32%

Table 10: Adaptive metamorphic testing of forward fitness scores and BD scores from Xie et al. [38]: the first column specifies the data, model, pseudo-accuracy, and underlying data transformations. The second column specifies which metric is used for testing. The rest of the columns are the pseudo-accuracy of tests prioritized by each metric during each iteration in adaptive testing and the accuracy is relative to pseudo-labels rather than ground-truth labels.

Data Model Pseudo-accuracy Transformations	Fitness	Iter 1	Iter 2	Iter 3	Iter 4	Iter 5
MNIST LeNet-1 100% Natural	FM	10.19%	0.22%	0.10%	0.10%	0.09%
	FL	10.25%	0.23%	0.07%	0.07%	0.07%
	BM	32.56%	12.46%	4.28%	2.48%	1.82%
	BL	45.47%	18.79%	7.97%	4.44%	2.81%
	BD	25.93%	15.78%	13.32%	12.85%	12.62%
	BD-F	22.75%	7.36%	3.51%	2.83%	2.64%
MNIST LeNet-5 100% Natural	FM	8.65%	0.10%	0.01%	0.00%	0.00%
	FL	8.72%	0.12%	0.01%	0.00%	0.00%
	BM	32.41%	10.84%	4.43%	2.61%	1.41%
	BL	41.71%	14.75%	5.34%	2.89%	1.68%
	BD	29.37%	12.71%	9.81%	9.06%	8.43%
	BD-F	18.53%	5.01%	2.39%	1.90%	1.57%
SVHN ResNet-9 100% Natural	FM	18.47%	2.24%	0.72%	0.51%	0.45%
	FL	18.68%	2.45%	0.88%	0.67%	0.53%
	BM	76.85%	54.48%	39.45%	29.22%	21.46%
	BL	78.13%	57.59%	42.78%	32.56%	24.09%
	BD	37.93%	14.76%	10.66%	10.11%	10.02%
	BD-F	21.74%	4.31%	2.07%	1.46%	1.19%
SVHN VGG 100% Natural	FM	19.61%	4.58%	3.19%	2.80%	2.46%
	FL	19.67%	4.99%	3.70%	3.27%	2.89%
	BM	72.54%	48.12%	33.80%	24.93%	19.14%
	BL	73.66%	50.23%	35.84%	26.55%	20.33%
	BD	29.92%	18.82%	19.59%	19.76%	19.84%
	BD-F	21.35%	6.48%	4.83%	4.20%	3.80%

Table (Continued)

CIFAR10 ResNet-18 100% Natural	FM	11.43%	1.69%	0.86%	0.60%	0.40%
	FL	11.56%	1.83%	0.94%	0.69%	0.53%
	BM	76.11%	59.72%	46.11%	37.77%	31.57%
	BL	76.13%	59.95%	46.77%	38.24%	31.83%
	BD	23.77%	13.20%	12.37%	12.34%	12.37%
	BD-F	15.79%	3.78%	2.27%	1.80%	1.51%
CIFAR10 VGG 100% Natural	FM	9.14%	1.64%	0.83%	0.71%	0.62%
	FL	9.14%	1.70%	0.93%	0.83%	0.76%
	BM	73.25%	56.16%	43.35%	34.75%	29.28%
	BL	74.21%	57.81%	45.44%	36.93%	30.57%
	BD	16.05%	9.83%	9.62%	9.38%	9.39%
	BD-F	11.13%	3.03%	1.91%	1.57%	1.33%
CIFAR100 ResNet-18 100% Natural	FM	3.53%	0.24%	0.13%	0.08%	0.07%
	FL	4.01%	0.31%	0.15%	0.09%	0.07%
	BM	52.02%	34.72%	23.43%	16.88%	13.20%
	BL	53.22%	35.69%	24.87%	17.91%	14.40%
	BD	9.31%	1.44%	1.17%	1.13%	1.17%
	BD-F	5.09%	0.54%	0.34%	0.26%	0.20%
CIFAR100 VGG 100% Natural	FM	3.36%	0.33%	0.19%	0.12%	0.11%
	FL	3.41%	0.34%	0.19%	0.14%	0.11%
	BM	50.66%	33.25%	22.13%	16.04%	12.16%
	BL	52.02%	35.26%	23.97%	17.46%	13.71%
	BD	6.75%	1.14%	0.94%	0.86%	0.83%
	BD-F	4.44%	0.53%	0.21%	0.16%	0.16%

Table 11: Adaptive metamorphic testing of forward fitness scores and BD scores from Xie et al. [38]: the first column specifies the data, model, pseudo-accuracy, and underlying data transformations. The second column specifies which metric is used for testing. The rest of the columns are the pseudo-accuracy of tests prioritized by each metric during each iteration in adaptive testing and the accuracy is relative to pseudo-labels rather than ground-truth labels.

Data Model Pseudo-accuracy Transformations	Fitness	Iter 1	Iter 2	Iter 3	Iter 4	Iter 5
MNIST LeNet-1 100% SD	FM	98.09%	95.87%	93.50%	90.45%	86.91%
	FL	98.14%	96.03%	93.61%	90.74%	87.35%
	BM	70.21%	15.51%	2.37%	0.20%	0.04%
	BL	33.03%	0.65%	0.00%	0.00%	0.00%
	BD	99.59%	99.41%	99.22%	98.81%	98.50%
	BD-F	99.58%	99.28%	98.99%	98.68%	98.14%
MNIST LeNet-5 100% SD	FM	98.94%	97.72%	96.32%	94.46%	91.44%
	FL	98.96%	97.75%	96.39%	94.60%	91.66%
	BM	69.05%	13.69%	1.41%	0.04%	0.00%
	BL	42.05%	1.39%	0.01%	0.00%	0.00%
	BD	99.75%	99.58%	99.51%	99.43%	99.26%
	BD-F	99.69%	99.36%	99.03%	98.42%	97.77%
SVHN ResNet-9 100% SD	FM	99.32%	98.69%	98.09%	97.47%	96.79%
	FL	99.34%	98.72%	98.16%	97.57%	96.92%
	BM	90.40%	78.22%	64.22%	50.72%	39.14%
	BL	87.32%	71.41%	54.93%	41.11%	29.95%
	BD	99.91%	99.84%	99.78%	99.75%	99.69%
	BD-F	99.82%	99.71%	99.56%	99.47%	98.35%
SVHN VGG 100% SD	FM	99.33%	98.50%	97.89%	97.21%	96.55%
	FL	99.35%	98.51%	97.91%	97.25%	96.61%
	BM	86.33%	73.89%	63.21%	53.46%	44.40%
	BL	85.79%	72.11%	60.05%	49.18%	39.51%
	BD	99.80%	99.61%	99.41%	99.17%	98.94%
	BD-F	99.70%	99.34%	99.07%	98.71%	98.44%
CIFAR10 ResNet-18 100% SD	FM	98.05%	96.21%	94.17%	92.56%	90.94%
	FL	98.14%	96.30%	94.22%	92.72%	91.11%
	BM	68.20%	42.29%	26.16%	15.67%	9.58%
	BL	65.08%	37.18%	20.81%	10.94%	6.08%
	BD	99.57%	99.31%	99.04%	98.80%	98.46%
	BD-F	99.25%	98.76%	98.15%	97.59%	97.18%

Table (Continued)

CIFAR10 VGG 100% SD	FM	98.69%	97.00%	95.55%	94.29%	92.71%
	FL	98.71%	97.00%	95.63%	94.33%	92.74%
	BM	71.34%	50.70%	36.72%	26.69%	18.88%
	BL	70.38%	48.72%	34.28%	24.23%	16.55%
	BD	99.53%	98.90%	98.38%	97.93%	97.56%
	BD-F	99.36%	98.67%	97.94%	97.29%	96.68%
CIFAR100 ResNet-18 100% SD	FM	91.76%	84.64%	78.53%	73.55%	69.12%
	FL	93.25%	86.99%	81.70%	77.04%	72.67%
	BM	38.38%	14.01%	4.48%	1.53%	0.58%
	BL	34.31%	11.40%	3.54%	1.22%	0.42%
	BD	98.12%	96.74%	95.74%	94.98%	94.19%
	BD-F	96.88%	94.65%	92.38%	90.30%	88.11%
CIFAR100 VGG 100% SD	FM	93.46%	88.32%	83.45%	79.25%	75.41%
	FL	93.76%	88.78%	84.11%	79.94%	76.08%
	BM	43.49%	21.97%	11.42%	5.74%	3.02%
	BL	38.36%	17.98%	8.43%	3.86%	2.06%
	BD	98.19%	97.25%	96.13%	95.26%	94.45%
	BD-F	97.24%	95.07%	92.98%	90.91%	89.10%

Table 12: Adaptive metamorphic testing of forward fitness scores and BD scores from Xie et al. [38]: the first column specifies the data, model, pseudo-accuracy, and underlying data transformations. The second column specifies which metric is used for testing. The rest of the columns are the pseudo-accuracy of tests prioritized by each metric during each iteration in adaptive testing and the accuracy is relative to pseudo-labels rather than ground-truth labels.

Data Model Pseudo-accuracy Transformations	Fitness	Iter 1	Iter 2	Iter 3	Iter 4	Iter 5
MNIST LeNet-1 100% Mixed	FM	6.28%	0.23%	0.06%	0.00%	0.00%
	FL	6.39%	0.25%	0.06%	0.00%	0.00%
	BM	29.37%	11.12%	5.70%	2.43%	1.51%
	BL	42.11%	18.20%	10.31%	5.86%	3.63%
	MM	6.27%	0.17%	0.01%	0.00%	0.00%
	ML	6.33%	0.09%	0.00%	0.00%	0.00%
	BD	20.58%	15.85%	14.35%	13.79%	13.20%
	BD-F	16.21%	7.87%	4.86%	3.83%	2.98%
MNIST LeNet-5 100% Mixed	FM	4.39%	0.04%	0.00%	0.00%	0.00%
	FL	4.41%	0.04%	0.00%	0.00%	0.00%
	BM	31.55%	9.91%	4.50%	2.08%	1.20%
	BL	40.98%	15.41%	6.71%	3.20%	1.62%
	MM	4.37%	0.04%	0.00%	0.00%	0.00%
	ML	4.37%	0.03%	0.00%	0.00%	0.00%
	BD	23.07%	13.01%	11.13%	10.85%	10.58%
	BD-F	13.27%	5.42%	3.90%	3.13%	2.77%
SVHN ResNet-9 100% Mixed	FM	13.86%	1.41%	0.30%	0.05%	0.02%
	FL	14.06%	1.67%	0.42%	0.05%	0.02%
	BM	78.68%	54.53%	35.91%	23.67%	15.98%
	BL	76.68%	49.62%	29.66%	17.04%	10.16%
	MM	13.35%	0.69%	0.05%	0.00%	0.00%
	ML	13.21%	0.65%	0.04%	0.01%	0.00%
	BD	32.21%	14.87%	11.07%	10.49%	10.54%
	BD-F	16.96%	3.33%	1.51%	0.85%	0.63%
SVNH VGG 100% Mixed	FM	15.00%	3.76%	2.47%	2.06%	1.82%
	FL	15.07%	4.31%	3.04%	2.56%	2.31%
	BM	72.28%	48.64%	32.46%	21.00%	13.89%
	BL	73.89%	50.65%	32.99%	20.39%	12.55%
	MM	13.96%	0.40%	0.01%	0.01%	0.00%
	ML	13.90%	0.48%	0.03%	0.01%	0.00%
	BD	26.36%	19.38%	19.69%	19.81%	19.84%
	BD-F	16.77%	5.81%	4.29%	3.67%	3.30%

Table (Continued)

CIFAR10 ResNet-18 100% Mixed	FM	8.93%	1.06%	0.26%	0.15%	0.10%
	FL	9.06%	1.14%	0.34%	0.19%	0.12%
	BM	58.04%	32.13%	18.93%	12.58%	8.82%
	BL	53.43%	24.31%	10.65%	4.86%	2.14%
	MM	7.15%	0.36%	0.05%	0.01%	0.00%
	ML	7.03%	0.33%	0.04%	0.00%	0.00%
	BD	20.66%	13.00%	12.48%	12.76%	12.64%
	BD-F	13.08%	3.42%	2.22%	1.68%	1.36%
CIFAR10 VGG 100% Mixed	FM	7.04%	1.64%	1.07%	0.80%	0.60%
	FL	7.05%	1.68%	1.16%	0.96%	0.88%
	BM	62.62%	40.87%	26.85%	18.30%	12.16%
	BL	61.87%	38.33%	22.66%	13.33%	7.64%
	MM	5.29%	0.42%	0.10%	0.00%	0.00%
	ML	5.22%	0.43%	0.08%	0.01%	0.00%
	BD	15.54%	9.71%	9.60%	9.61%	9.63%
	BD-F	9.10%	3.08%	2.21%	1.73%	1.46%
CIFAR100 ResNet-18 100% Mixed	FM	2.60%	0.21%	0.07%	0.03%	0.01%
	FL	2.94%	0.33%	0.12%	0.04%	0.03%
	BM	28.65%	12.03%	8.27%	5.77%	3.53%
	BL	23.28%	4.82%	1.48%	0.71%	0.52%
	MM	1.80%	0.01%	0.00%	0.00%	0.00%
	ML	1.91%	0.02%	0.00%	0.00%	0.00%
	BD	6.88%	1.49%	1.24%	1.18%	1.16%
	BD-F	3.97%	0.69%	0.42%	0.27%	0.26%
CIFAR100 VGG 100% Mixed	FM	2.31%	0.27%	0.09%	0.05%	0.03%
	FL	2.33%	0.28%	0.11%	0.05%	0.04%
	BM	36.10%	17.51%	9.48%	6.57%	4.39%
	BL	29.46%	11.30%	4.33%	2.36%	1.46%
	MM	1.82%	0.08%	0.01%	0.01%	0.00%
	ML	1.78%	0.05%	0.01%	0.01%	0.01%
	BD	5.28%	1.01%	0.89%	0.89%	0.87%
	BD-F	3.03%	0.42%	0.17%	0.15%	0.12%

Table 13: Adaptive testing of forward fitness scores and BD scores from Xie et al. [38] for 3 iterations: the first column specifies the data, model, clean accuracy, and underlying data transformations. The second column specifies which metric is used for testing. The rest of the columns are the accuracy of tests prioritized by each metric during each iteration in adaptive testing.

Data, Model, Accuracy, Transformations	Fitness	Iter 1	Iter 2	Iter 3
MNIST,	FM	4.67%	0.01%	0.00%
LeNet-5,	FL	4.73%	0.01%	0.00%
99.01%,	BD	21.50%	10.90%	8.88%
Benign	BD-F	13.51%	3.69%	2.09%
SVHN,	FM	9.27%	0.81%	0.23%
ResNet-9,	FL	9.47%	0.93%	0.32%
95.90%,	BD	28.02%	13.10%	10.79%
Benign	BD-F	12.41%	2.68%	1.49%
CIFAR10,	FM	5.44%	0.84%	0.47%
VGG,	FL	5.50%	0.88%	0.53%
91.48%,	BD	13.97%	9.68%	9.42%
Benign	BD-F	8.49%	2.35%	1.64%
CIFAR100,	FM	1.82%	0.15%	0.03%
ResNet-18,	FL	2.03%	0.20%	0.05%
70.45%,	BD	5.08%	1.34%	1.13%
Benign	BD-F	2.66%	0.41%	0.22%

Table 14: Adaptive testing of forward fitness scores and BD scores from Xie et al. [38] for 8 iterations: the first column specifies the data, model, clean accuracy, and underlying data transformations. The second column specifies which metric is used for testing. The rest of the columns are the accuracy of tests prioritized by each metric during each iteration in adaptive testing.

Data, Model, Accuracy, Transformations	Fitness	Iter 1	Iter 2	Iter 3	Iter 4	Iter 5	Iter 6	Iter 7	Iter 8
MNIST,	FM	8.36%	0.15%	0.0%	0.0%	0.0%	0.0%	0.0%	0.0%
LeNet-5,	FL	8.38%	0.16%	0.0%	0.0%	0.0%	0.0%	0.0%	0.0%
99.01%,	BD	31.11%	12.80%	10.53%	9.66%	8.92%	8.58%	8.53%	8.56%
Benign	BD-F	14.28%	2.87%	2.04%	1.78%	1.43%	1.32%	1.23%	1.15%
SVHN,	FM	17.16%	1.86%	0.54%	0.35%	0.30%	0.28%	0.27%	0.25%
ResNet-9,	FL	17.35%	2.05%	0.66%	0.43%	0.35%	0.32%	0.29%	0.29%
95.90%,	BD	36.73%	14.34%	10.53%	9.92%	9.83%	9.80%	9.85%	9.84%
Benign	BD-F	20.76%	4.22%	2.00%	1.52%	1.29%	1.19%	1.09%	1.03%
CIFAR10,	FM	9.41%	1.33%	0.74%	0.59%	0.51%	0.46%	0.41%	0.35%
VGG,	FL	9.44%	1.46%	0.86%	0.73%	0.64%	0.58%	0.52%	0.45%
91.48%,	BD	17.26%	9.99%	9.72%	9.56%	9.49%	9.46%	9.43%	9.44%
Benign	BD-F	13.25%	3.40%	2.45%	2.02%	1.88%	1.67%	1.50%	1.34%
CIFAR100,	FM	3.69%	0.31%	0.06%	0.04%	0.02%	0.01%	0.00%	0.00%
ResNet-18,	FL	4.10%	0.35%	0.11%	0.07%	0.03%	0.02%	0.01%	0.01%
70.45%,	BD	9.22%	1.26%	1.07%	1.04%	1.05%	1.02%	1.01%	0.98%
Benign	BD-F	5.68%	0.64%	0.44%	0.34%	0.26%	0.27%	0.25%	0.25%